Gap Junctions in the Inner Ear: Comparison of Distribution Patterns in Different Vertebrates and Assessment of Connexin Composition in Mammals

ARTICLE *in* THE JOURNAL OF COMPARATIVE NEUROLOGY · DECEMBER 2003

Impact Factor: 3.23 · DOI: 10.1002/cne.10916 · Source: PubMed

6 AUTHORS, INCLUDING:

David L Becker
Nanyang Technological University
138 PUBLICATIONS **4,157** CITATIONS
SEE PROFILE

Stefano Casalotti
University of East London
33 PUBLICATIONS **985** CITATIONS
SEE PROFILE

THE JOURNAL OF COMPARATIVE NEUROLOGY 467:207–231 (2003)

Gap Junctions in the Inner Ear: Comparison of Distribution Patterns in Different Vertebrates and Assessement of Connexin Composition in Mammals

ANDREW FORGE,[1]* DAVID BECKER,[2] STEFANO CASALOTTI,[1] JILL EDWARDS,[1] NERISSA MARZIANO,[1] AND GRAHAM NEVILL[1]
[1]UCL Centre for Auditory Research and Institute of Laryngology and Otology, University College London, London WC1X 8EE, United Kingdom
[2]Department of Anatomy and Developmental Biology, University College London, London WC1E 6BT, United Kingdom

ABSTRACT

The distribution and size of gap junctions (GJ) in the sensory epithelia of the inner ear have been examined in a reptile (gecko), birds (chicken and owl), and mammals (mouse, guinea pig, gerbil, and bat), and the connexin composition of GJs in the mammalian inner ear has been assessed. Freeze fracture revealed a common pattern of GJ distribution in auditory and vestibular sensory epithelia in the different vertebrate classes. In all these tissues, GJs are numerous, often occupying more than 25% of the plasma membrane area of supporting cells and sometimes composed of more than 100,000 channels. Screening for 12 members of the connexin family in the mammalian inner ear by RT-PCR, Western blotting, and immunohistochemistry revealed four connexin isotypes, cx26, cx30, cx31, and cx43, in the cochlea and three, cx26, cx30, and cx43, in the vestibular organs. With antibodies characterised for their specificity, cx26 and cx30 colocalised in supporting cells of the organ of Corti, in the basal cell region of the stria vascularis, and in type 1 fibrocytes of the spiral ligament. No other connexin was detected in these regions. Cx31 was localised among type 2 fibrocytes below the spiral prominence, a region where cx30 was not expressed and cx26 expression appeared to be low. Cx43 was detected only in the region of "tension fibrocytes" lining the inner aspect of the otic capsule. This suggests separate functional compartments in the cochlea. In addition to cx26 and cx30, cx43 was detected in supporting cells of the vestibular sensory epithelia. Where cx26 and cx30 were colocalised, double immunogold labelling of thin sections showed both cx26 and cx30 evenly distributed in individual GJ plaques, a pattern consistent with the presence of heteromeric connexons. Coimmunoprecipitation of cochlear membrane proteins solubilised with a procedure that preserves the oligomeric structure of connexons confirmed the presence of heteromeric cx26/cx30 connexons. Heteromeric cx26/cx30 connexons may be unique to the inner ear, which could be one factor underlying the non-syndromic character of the deafness caused by mutations in cx26. J. Comp. Neurol. 467: 207–231, 2003.

Indexing terms: heteromeric connexons; cx26; cx30; annular gap junctions; hereditary deafness; cochlea; vestibular system

Grant sponsor: the Wellcome Trust; Grant number: 056611; Grant sponsor: the Golden Charitable Trust and Defeating Deafness.

Nerissa Marziano's current address is Department of Biosciences, University of Kent at Canterbury, Canterbury, Kent CT2 7NJ, United Kingdom.

*Correspondence to: Andrew Forge, UCL Centre for Auditory Research and Institute of Laryngology and Otology, University College London, 330-332 Gray's Inn Road, London WC1X 8EE, United Kingdom. E-mail: a.forge@ucl.ac.uk

Received 23 May 2003; Revised 17 July 2003; Accepted 17 July 2003

DOI 10.1002/cne.10916

Published online the week of October 20 2003 in Wiley InterScience (www.interscience.wiley.com).

Gap junctions are sites of direct communication between cells where channels through the plasma membrane of one cell are in direct register with similar channels through the membrane of its neighbour to form continuous aqueous pores linking the cytoplasmic compartments. The channels allow the passage of ions and small metabolites up to a size of ~1,200 Da, coupling cells electrically and chemically (Gilula et al., 1972; Kumar and Gilula, 1996; Evans and Martin, 2002; Willecke et al., 2002). The channel unit of an individual cell, the gap junction "hemichannel," is called a *connexon*. Connexons are aggregated in the plane of the membrane, creating distinct macromolecular assemblies that are most easily visualised by freeze fracture, which exposes face views of membranes. Gap junctions are then seen as two-dimensionally extensive plaques of closely packed particles, the particles representing the connexons (McNutt and Weinstein, 1970; Severs, 1990). The size and shape of individual gap junction plaques, and the number of channels they comprise, can be determined using freeze fracture.

A connexon is formed by oligomerisation of six connexin protein molecules. The connexins are a family of related proteins. The genes for 20 different connexins are present in the human genome and 19 in that of the mouse (Evans and Martin, 2002; Willecke et al., 2002). The protein products of the different connexin genes vary in molecular weight, from which they derive their common names [connexin 26 (cx26), cx30, etc.], but they are topologically similar (Kumar and Gilula, 1996; Evans and Martin, 2002). They possess four intramembrane regions, two extracellular loops, and a cytoplasmic loop, and both the N- and C-termini are cytoplasmic. Variations in the sequences of the different connexin proteins occur mainly in the C-terminal tail and in the cytoplasmic loop. Antibodies raised to epitopes within these regions provide labels to identify the different connexins. The particular physiological characteristics of the individual connexins have not been fully elucidated, but the connexins differ in the size and charge characteristics of the channel and in their regulatory properties (Veenstra, 1996; Evans and Martin, 2002). Many, perhaps most, cells that form gap junctions express more than one connexin isoform, and this can result in a variety of connexin and connexon arrangements (Kumar and Gilula, 1996). Connexons may be homomeric or heteromeric (more than one type of connexin within an individual connexon); junctions can be homotypic or heterotypic (the connexin composition of connexons of one cell are different from those of the neighbour to which it is coupled); a cell may traffic different connexins to different locations so that the gap junctions formed with one cell are different in composition from those formed with another neighbour; and separate islands of homomeric-homotypic connexons can be present within the same gap junction plaque (Falk, 2000). These differing arrangements will result in gap junctions with distinct properties (Bruzzone et al., 1996; Evans and Martin, 2002).

Freeze-fracture studies have shown gap junctions to be numerous in the tissues of the inner ear (Jahnke, 1975; Gulley and Reese, 1976; Iurato et al., 1976, 1977; Ginzberg and Gilula, 1979; Hirokawa, 1980; Forge, 1984, 1986; Forge et al., 1999). Their importance to auditory function has been emphasised by the findings that mutations in the genes for four different connexins, cx26, cx30, cx31, and cx43, cause hereditary hearing loss (Carrasquillo et al., 1997; Denoyelle et al., 1997; Kelsell et al., 1997; Xia et al., 1998; Grifa et al., 1999; Kelley et al., 2000; Liu et al., 2001; Bitner-Glindzicz, 2002). Deafness is also associated with x-linked Charcot-Marie-Tooth disease (CMTX; Kousseff et al., 1982; Hamiel et al., 1993), which results from mutation in the gene for cx32 (Scherer et al., 1999). Mutations in the gene for Cx26 (*GJB2*) are now recognised as the most common cause of congenital, nonsyndromic deafness (Bitner-Glindzicz, 2002). Cx26 is widely expressed in the cochlea and the vestibular system (Kikuchi et al., 1994, 1995; Forge et al., 1999, 2002). Cx30 is also expressed extensively, and its localisation may overlap with that of cx26 (Lautermann et al., 1998, 1999; Xia et al., 2001; Forge et al., 2002), but whether the two connexons are present in the same gap junction plaques and, if so, whether they form heteromeric connexons or heterotypic junctions have not been determined.

The roles that gap junctions play in the inner ear have not been defined. It has been proposed that one function may be to provide an intracellular route to ferry K^+ ions away from the sensory cells during auditory transduction to maintain signal sensitivity (Kikuchi et al., 1995, 2000; Forge et al., 1999; Wangemann, 2002). The sensory epithelia of the inner ear are composed of sensory "hair" cells and nonsensory supporting cells, each hair cell surrounded by supporting cells. The apical surface of the epithelium is bathed in a K^+-rich fluid, endolymph, and a K^+ current passes through the hair cell along an electrochemical gradient. When hair cells are stimulated, the current flow is modulated, the consequent changes in membrane potential generating hair cell responses. Maintenance of the low-K^+ environment around the basolateral surface of the supporting cell is therefore of importance. It is suggested that supporting cells take up K^+, perhaps through the action of the K-Cl cotransporter Kcc4 (Boettger et al., 2002), with gap junctions providing the route through which it is ferried away from the sites of transduction to maintain the ionic environment around the hair cell. Gap junctions may also be involved in a pathway for recycling K^+ back to endolymph, and, in the cochlea, but not the vestibular system, this may be associated with the generation of a high positive resting potential, the endocochlear potential (EP) of approximately +80 mV that is present in the cochlear endolymphatic compartment (Kikuchi et al., 1995; Souter and Forge, 1998; Wangemann, 2002). Gap junctions may therefore be important for the generation and maintenance of EP by the stria vascularis, the ion-transporting epithelium of the cochlea, which lines the lateral wall of the endolymphatic compartment. Numerous gap junctions are associated with one cell type in the stria, the basal cells (Forge, 1984; Carlisle et al., 1990; Souter and Forge, 1998), which separate the stria from the underlying spiral ligament. Strial basal cells form gap junctions with ligament fibrocytes and fibrocytes are rich in Na^+/K^+-ATPase (McGuirt and Schulte, 1994; Schulte and Steel, 1994). Thus, gap junctions could provide a route for transport of K^+ from ligament fibrocytes into the stria that bypasses the tight junction network between basal cells that prevents passive diffusion between stria and ligament (Forge, 1981, 1984; Souter and Forge, 1998). There is, however, as yet no direct evidence for a role of gap junctions in the potassium recycling in the inner ear, but mice with a deletion of cx30 are deaf and do not generate an EP (Teubner et al., 2003).

Deletion of cx30 also results in death of outer hair cells. Death of outer hair cells, initiated at about the time of the onset of hearing, is also a consequence of targeted deletion of cx26 from the supporting cells of the organ of Corti (Cohen-Salmon et al., 2002) and of expression in mice of a dominant negative mutation in cx26, R75W, that causes deafness in humans (Kudo et al., 2003). These observations suggest that maintenance of homeostasis is particularly important for hair cell survival in the cochlea and that, at least in the organ of Corti, cx26 and cx30 may not be able to compensate for each other should either be defective.

To construct realistic physiological models of how intercellular communication via gap junctions maintains inner ear function, a knowledge of how gap junctions are distributed, their relative sizes and numbers, and the connexin composition of their connexons is required. As a first step toward that goal, in the present work we have used freeze fracture to determine the distribution and relative sizes of gap junction plaques in the inner ear tissues of a number of different vertebrates in order to identify commonalities and differences between species and between auditory and vestibular sensory epithelia. We have analysed, in the mammalian inner ear, which connexins are expressed in the sensory epithelia and stria vascularis and have used immunogold labelling and immunoprecipitation to identify the composition and distribution of connexins in individual gap junction plaques.

MATERIALS AND METHODS

Freeze fracture

Freeze-fracture analysis of gap junctions was carried out for mammals, birds, and reptiles using the cochlear tissues from guinea pigs, gerbils, mice, and moustached bats and the basilar papillae of chickens, barn owls, and geckos. Vestibular tissues of mice, guinea pigs, chicks, and owls were also examined. Pigmented guinea pigs, gerbils (*Meriones unguiculatus*), and mice (CBA/CA strain) were from our own breeding stocks. Bat (*Pteronotus parnellii*) cochleae were provided by Dr. Marianne Vater (University of Dresden). The basilar papillae from 7-day-old chickens were supplied by Dr. Yehoash Raphael (University of Michigan), those from adult barn owls by Dr. Christine Koppl (Technical University, Munich), and those from geckos (*Gekko gecko*) by Prof. Geoff Manley (Technical University, Munich). All animal work was conducted under licensed procedures of the British Home Office and with approval of the UCL Animal Ethics Committee.

Inner ears were isolated and fixed directly in 2.5% glutaraldehyde in 0.1 M cacodylate buffer with 3 mM $CaCl_2$, pH 7.3, for 1.5 hours, then transferred to 0.1 M cacodylate buffer. The organs of Corti and lateral wall tissues were dissected from the mammalian cochleae, the basilar papillae from those of the birds and reptiles. Utricles and cristae were taken from the mammals and birds. The tissues were infiltrated with 25% glycerol in 0.1 M cacodylate buffer for 45–60 minutes, before being mounted on specimen holders and frozen in propane:isopentane (4:1) cooled in liquid nitrogen. Fracture was performed on a Balzers BAF400 device by using standard procedures.

TABLE 1. Primers Used for All Connexins

Cx	Forward	Reverse
26	TTCAGACCTGCTCCTTACCG	GGAAGTGGTGGTCGTAGCAT
30	AGGAAGTGTGGGGTGATGAG	AGGTAACACAACTCGGCCAC
30.3	TCAAACATGGGCCCAATG	GGGAGTCACAGAGCAAGC
31	AGAAGCACGGGGAGCAAT	TACTATGCTGGCGCACTG
32	CAGACACGCCTGCATACATT	CCTCAAGCCGTAGCATTTTC
37	GGCTGGACCATGGAGCCGGT	TTTCGGCCACCCTGGGGGGC
43	AATGAGGCAGGATGAACTGG	CATGAAGACAGCCTCGAACA
45	AATGCTAAGATTGCCTACA	CCCCTGATTTGCTACTAA
47	AACGTCTGCTATGACGCCTT	GGCAGCTGACCACGTACATA
50	CATCCTGCCCCTCTATC	CTCTTCCCGCTCCACTT

Reverse Transcription-Polymerase Chain Reaction

Reverse transcription-polymerase chain reaction (RT-PCR) was used to screen for connexins expressed in the inner ears of mature mice, 6–8 weeks old. For each preparation, 8–10 auditory bullae were dissected on ice. The cochlear and vestibular tissues were collected separately. Pieces of mouse brain, heart, kidney, liver, and skin were taken for positive controls. RNA was extracted by standard procedures. Oligonucleotide primers for five connexins, cx26, cx30, cx32, cx43, and cx47, were designed with the Primer 3 program. Primers for a further five connexins, cx30.3, cx31, cx37, cx45, and cx50, were constructed according to published data (Davies et al., 1996). Alignments were performed on each set of primers with all connexin isoforms to exclude cross-reactivity. The forward and reverse primers are given in Table 1.

Three microliters of RNA solution and 1 μl of each of the primers were diluted in 5 μl nuclease-free water, to which was added 0.15 μl of Taq polymerase diluted in 10.1 μl nuclease-free water, with 2.5 μl chloride-free buffer, $MgCl_2$, 0.5 μl DNTP, and 0.25 μl AMV. For negative controls, 3 μl of nuclease-free water replaced the RNA solution. RNA encoding GAPDH was included in all PCR runs as a positive control. Samples were denatured at 94°C for 2 minutes, followed by 35 PCR cycles at 94°C for 30 seconds, annealing at 60°C for 30 seconds, strand synthesis at 72°C for 45 seconds, and final extension at 72°C for 7 minutes. Products were electrophoresed on 1.8% agarose gel with ethidium bromide at 80 mV for 1 hour.

Western blotting

Western blotting was used to confirm expression of connexin proteins in the inner ears of mature mice. Tissue from 8–10 auditory bullae was homogenised in $NaHCO_3$, 5 mM EDTA, 1 mM phenylmethylsulfonyl fluoride (PMSF), 1 mM orthovanadate, and 10 mM NaF. Homogenates of mouse heart, liver, kidney, skin, and eye tissues were prepared to serve as positive controls as appropriate for particular connexins. To an aliquot of homogenate an equal volume of sample buffer [100 mM Tris base, 20% glycerol, 4% sodium dodecyl sulfate (SDS), 10% 2-mercaptoethanol, 0.2% bromophenol blue, pH 6.8] was added. The mixture was sonicated briefly, then centrifuged to remove cell debris. The proteins in samples of the supernatant (10 μl) were resolved by polyacrylamide gel electrophoresis (at 100–150 V for 90–120 minutes) and transferred to nitrocellulose membranes (30 V overnight). The membranes were incubated in blocking solution [5% skimmed milk powder in Tris-buffered saline (TBS)] for 1 hour, then exposed to one of the anticonnexin primary

antibodies at dilutions in TBS of 1:1,000 to 1:5,000 for 1 hour at room temperature or overnight at 4°C. After several washes in TBS, the membranes were incubated in horseradish peroxidase (HRP)-conjugated secondary antibodies for 1 hour at room temperature. The blots were developed by using an ECL chemiluminescence kit (Amersham Pharmacia Biotech, Piscataway, NJ). The primary antibodies used were: to cx26, gap 28h polyclonal to residues in the cytoplasmic loop (gift from W.H. Evans, University of Wales College of Medicine) and β2J monoclonal to the cytoplasmic loop (gift from the late N.B. Gilula, The Scripps Research Institute [TSRI]); to cx30, polyclonal to the C-terminal tail (Zymed, South San Francisco, CA); to cx32, β1J polyclonal to C-terminal tail (TSRI); to cx43, α1S polyclonal to C-terminal tail (TSRI); to cx45, α6J to cytoplasmic loop (TSRI); to cx46, α3J to cytoplasmic loop (TSRI); and, to cx50, α8 monoclonal (TSRI).

Immunohistochemistry

Localisation of 10 different connexins, cx26, cx30, cx31, cx32, cx37, cx40, cx43, cx45, cx46, and cx50, was examined in frozen sections and whole-mount preparations of cochlear and vestibular tissues from adult mice and of cx26, cx30, cx32, and cx43 in guinea pigs and gerbils. Sections of brain, heart, lens, liver, kidney, and skin were also prepared for positive controls for the various connexins.

Inner ears were fixed directly in 4% freshly prepared paraformaldehyde for 1 hour at room temperature, in methanol followed by acetone at –20°C, or in ethanol. For whole-mount preparations, and for frozen sections from guinea pigs and gerbils, the tissues were then dissected out under phosphate-buffered saline (PBS). For frozen sections from the mice, the bullae were first decalcified in either 4.13% EDTA, pH 7.5, for 2 days at 4°C or 1% ascorbic acid, 0.8% NaCl for 7 days, with changes of solution every 2 days (Merchan-Perez et al., 1999). Samples for frozen sections were incubated overnight in 30% sucrose in PBS, then embedded in 1% low-gelling-temperature agarose in 18% sucrose in PBS at 37°C. The agarose tissue blocks were mounted on chucks in OCT compound and frozen in liquid nitrogen. Sections were cut at 10–15 μm and mounted on polylysine-coated slides. Tissue sections or tissues prepared for whole mounts were permeabilised in 0.5% Triton X-100 for 15 minutes, then incubated in a block solution (either 10% horse serum in PBS-0.05% Triton or 100 mM L-lysine, 10% dried skimmed milk powder), before incubation overnight at 4°C in primary anticonnexin antibody diluted 1:100 in block solution. After six washes in PBS, the tissues/sections were incubated in FITC-, TRITC-, or Alexa Fluo 633-conjugated anti-rabbit or anti-mouse secondary antibody diluted 1:100 or biotinylated goat anti-rabbit or anti-mouse secondary antibody (Dako, Carpinteria, CA; 1:150 in block solution) for 1.5 hours, washed, and then exposed to streptavidin-FITC (Dako; 1:150) for 1.5 hours. After thorough washes in PBS, the sections or whole-mount preparations on slides were coverslipped using an antifade compound [Slow Fade Light (Molecular Probes, Eugene, OR) or Vectashield (Vector Laboratories, Burlingame, CA)]. In some cases, phalloidin at 0.25 μg/ml was added to the secondary antibody solution. The primary antibody was omitted in negative controls. Specimens were examined by standard epifluorescence or by confocal microscopy (Leica).

The primary antibodies used were: to cx26, gap28H polyclonal and β2J monoclonal (as described above) and a polyclonal to the C-terminal tail (Zymed); to cx30, a polyclonal and a monclonal both from Zymed; to cx31, an anti-mouse polyclonal from K. Willecke, an anti-human polyclonal from D. Kelsell, β3s polyclonal from N.B Gilula, and a commercial polyclonal from Alpha Diagnostics; to cx32, β1J (as described above), Gap 2a monoclonal, Des 1 polyclonal, Des 5 polyclonal (to different epitopes in the cytoplasmic loop; all three from D. Becker), Gap 31h polyclonal to the amino terminal tail and Gap 34r polyclonal to the C-terminal tail (both from W.H. Evans); to cx37, a polyclonal Y16Y (from N. Severs, Imperial College) and a polyclonal from D. Becker; to cx40, S15C polyclonal (from N. Severs); to cx43: α1s polyclonal (from N.B. Gilula), Gap 1a monoclonal and Gap 15 polyclonal to the cytoplasmic loop (both from D. Becker), Gap 33r polyclonal to C-terminal tail (from W.H. Evans), and a monoclonal from Chemicon (Temecula, CA); to cx45, Q14E polyclonal to the c-terminal tail (from N. Severs) and α6J polyclonal to the cytoplasmic loop (from N.B. Gilula); to cx46, α3s polyclonal to C-terminal tail and α3J to the cytoplasmic loop (both from N.B. Gilula); and, to cx50, α8 monoclonal (from N.B. Gilula).

Immunogold labeling

Immunogold labeling was performed with cochlear and vestibular tissues of guinea pigs and mice. The inner ears were fixed directly in 2% paraformaldehyde, alone or supplemented with 0.025% glutaraldehyde, in PBS, pH 7.3, for 1 hour, then rinsed in PBS. Cochlear and vestibular tissues were isolated under PBS and dehydrated in an alcohol series before infiltration with LR Gold plastic. The plastic was polymerised with ultraviolet light at –30°C.

Thin sections were mounted on nickel grids and floated on a blocking solution (10% horse serum, 100 mM l-lysine in PBS with 0.15% Tween, pH 8.2) for 30 minutes. The sections were washed in several changes of PBS-0.15% Tween, pH 8.2, before overnight incubation at 4°C in primary antibody to cx26 or cx30 diluted 1:50 in PBS-Tween. The primary antibodies used were the rabbit polyclonal gap28H and the mouse monoclonal β2J to cx26 and the rabbit polyclonal to cx30 (Zymed). After labeling with the primary antibody, the sections were washed several times in PBS-Tween and then incubated for 1 hour at room temperature with a 1:50 dilution of the secondary antibody, conjugated to either 10-nm or 5-nm gold particles. They were rinsed in PBS and then in distilled water, allowed to dry, and then lightly counterstained with uranyl acetate and lead citrate.

Two different protocols were used to label the same junction plaque in thin sections of mouse inner ear tissues with the polyclonal antibodies. Successive, adjacent sections were separately labeled with anti-cx26 or anti-cx30. Each primary antibody was localised with a secondary coupled to 10-nm gold particles. Individual sections were also doubly labeled with the two polyclonal antibodies. With the sections mounted on a grid, after blocking, the grid was floated on the surface of a droplet of solution so that only one face of the section was exposed to one of the primary antibodies and then to the secondary antibody conjugated to 10-nm gold particles. The grid was washed several times by floating on droplets of distilled water, then turned over so that only the opposite face of the section was exposed to the second primary antibody and

then to the secondary antibody conjugated to 5-nm gold particles. Subsequent stereo-pair imaging revealed that the larger gold particles were confined to one face of the section, and the smaller gold particles to the other, confirming that each primary antibody was labeled separately (see Fig. 7D). Sections of guinea pig inner ear tissue were doubly labeled on the same face with the polyclonal to cx30 localised with a secondary conjugated to 10-nm gold particles and the monoclonal to cx26 localised with a secondary conjugated to 5-nm gold particles.

Labeling of connexins expressed in HeLa cells

Antibody specificity was tested by labeling cultured HeLa cells, which have no endogenous connexin expression (Elfgang et al., 1995), that had been transfected with cDNA for GFP (p-lantern; Promega, Madison, WI) and cDNA of either rat cx26 or mouse cx30. Full-length mouse cx26 cDNA cloned into pCR3 plasmid (Invitrogen, La Jolla, CA) was a gift from W.H. Evans (Cardiff, United Kingdom). cDNA for cx30 was generated by RT-PCR amplification of mouse heart mRNA with forward primer CGTAGAAGCTTGAATAAGCCTGCACGATGGAC and reverse primer CGTAGTCTAGAGCTCACCTACACTTGACCTTG containing flanking HindIII and XbaI restriction sites for directional cloning into pCR3 (Invitrogen). The sequence was confirmed to be identical to Genbank Z70023.

Plasmids were microinjected into the nuclei of HeLa cells (Ohio Strain 84121901 ECACC). Cells were incubated for a further 24 hours before fixation in 4% paraformaldehyde. Cells were labeled overnight at 4°C with either the gap28H cx26 antibody or the cx30 antibody, both used at 1:500 dilution, and then in rhodamine-conjugated anti-rabbit secondary antibody at 1:500 dilution for 2 hours at room temperature.

Immunoprecipitation

Cochleae from 8–10 adult mice were isolated on ice and homogenised in 500 μl of 20 mM triethanolamine (TEA), pH 9.2, containing 20 mM EDTA. The homogenate was centrifuged twice at 12,000*g*, with resuspension in 600 μl TEA buffer. To 180-μl aliquots of the resuspended homogenate, 20 μl of either 20% dodecyl maltoside (DM), which does not dissociate connexons (Stauffer et al., 1991), or 1% SDS was added to solubilise membrane proteins. Samples were sonicated for 5 minutes, incubated at 4°C for 60 minutes, then centrifuged at 12,000*g* for 5 minutes. The supernatant was diluted with 800 μl PBS, pH 7.4, containing either 0.5% DM or 0.1% Tween 20 for samples solubilised with DM and SDS, respectively. The solubilised proteins were then incubated at 4°C for 30 minutes with 50 μl protein G-sepharose beads (Pharmacia) resuspended in PBS, to remove nonspecific binding, then centrifuged at 8,000*g* for 2 minutes. The supernatant was collected and incubated at 4°C for 120 minutes with 2.5 μg polyclonal antibodies to either cx26 (Zymed) or cx30 (Zymed). After addition of 50 μl protein G-sepharose beads, incubation was continued at 4°C for 60 minutes to bind antibody-conjugated proteins. Samples were centrifuged and resuspended three times in PBS containing either 0.5% DM or 0.1% Tween 20. Finally, samples were resuspended in 30 μl electrophoresis sample buffer containing 1% SDS to solubilise bound proteins. Samples were electrophoresed on a Tri/Tricine electrophoresis system (Schagger and von Jagow, 1987) and blotted onto nitrocellulose paper (20 V, 4 hours). Nitrocellulose was incubated with 5% dry nonfat milk, 0.1% Tween 20 in PBS for 1 hour at room temperature. Strips of nitrocellulose sheets were individually incubated with monoclonal antibodies against cx26 (Zymed) or cx30 (Zymed; 1:500 in PBS, 0.1% Tween 20) for 90 minutes at room temperature. The nitrocellulose sheets were washed four times for 15 minutes each with PBS, 0.1% Tween and incubated with biotin conjugated anti-mouse antibodies (1:1,000 in PBS, 0.1% Tween 20) for 60 minutes at room temperature. After four further 15-minute washes, the nitrocellulose sheets were incubated with streptavidin-HRP (Zymed 1:5,000 in PBS, 0.1% Tween 20) for 60 minutes at room temperature and washed for 3 × 15 minutes in PBS with 0.1% Tween 20 and once for 15 minutes in PBS alone. The nitrocellulose sheets were developed according to the ECL method (Pharmacia).

Micrograph production

All images were prepared digitally using Adobe Photoshop 6.0 and adjusted only for optimal contrast and brightness.

RESULTS

Freeze fracture

Sensory epithelia. Gap junction plaques were never present on the plasma membrane faces of hair cells. They were, however, numerous and often very large on the plasma membranes of supporting cells in all species. In vestibular organs, gap junction plaques were present down the entire membrane face where supporting cells contact each other but were especially prevalent toward the lumenal membrane below the level of the tight junctions and around the cell body of the supporting cells. Detailed analysis of gap junction density and plaque sizes for a depth of ~8–10 μm from the lumenal surface and over a depth of 8–10 μm from the basement membrane over the cell body region was made in replicas of utricles of guinea pigs and mice. From junction size, the number of channels in each junction plaque was estimated using a figure of 12,500 channels/μm^2, determined from the number of connexon particles in 10 different junctions from 10 different replicas of fixed tissues. In the lumenal 10 μm depth of the epithelium, junctional plaques were numerous and often very small (Fig. 1A). They were present at a density of ~98/100 μm^2 (combined from measurements of 115 junctions in 24 micrographs from six replicas) and composed of between ~10 and 2,000 channels [mean of 362 ± 357 (SD), median 253, 115 junctions, >0.001 to ~0.17 μm^2 in area]. (For comparative purposes, these figures can be used to estimate a nominal, but biologically meaningless, channel density over the plasma membrane of ~350/μm^2). Around the body of the supporting cell, plaques were fewer, ~49/100 μm^2, but much larger (Fig. 1B), ranging in size from 550 to over 20,000 channels [mean 4,173 ± 4,761 (SD), median 4,960, 35 junctions from 22 micrographs of six different replicas, ~2,000 channels/μm^2 of plasma membrane]. A similar size distribution was evident in avian utricles: relatively larger numbers of smaller plaques similar in size to those in mammals toward the lumen and much larger plaques around the cell body region. These latter junction plaques

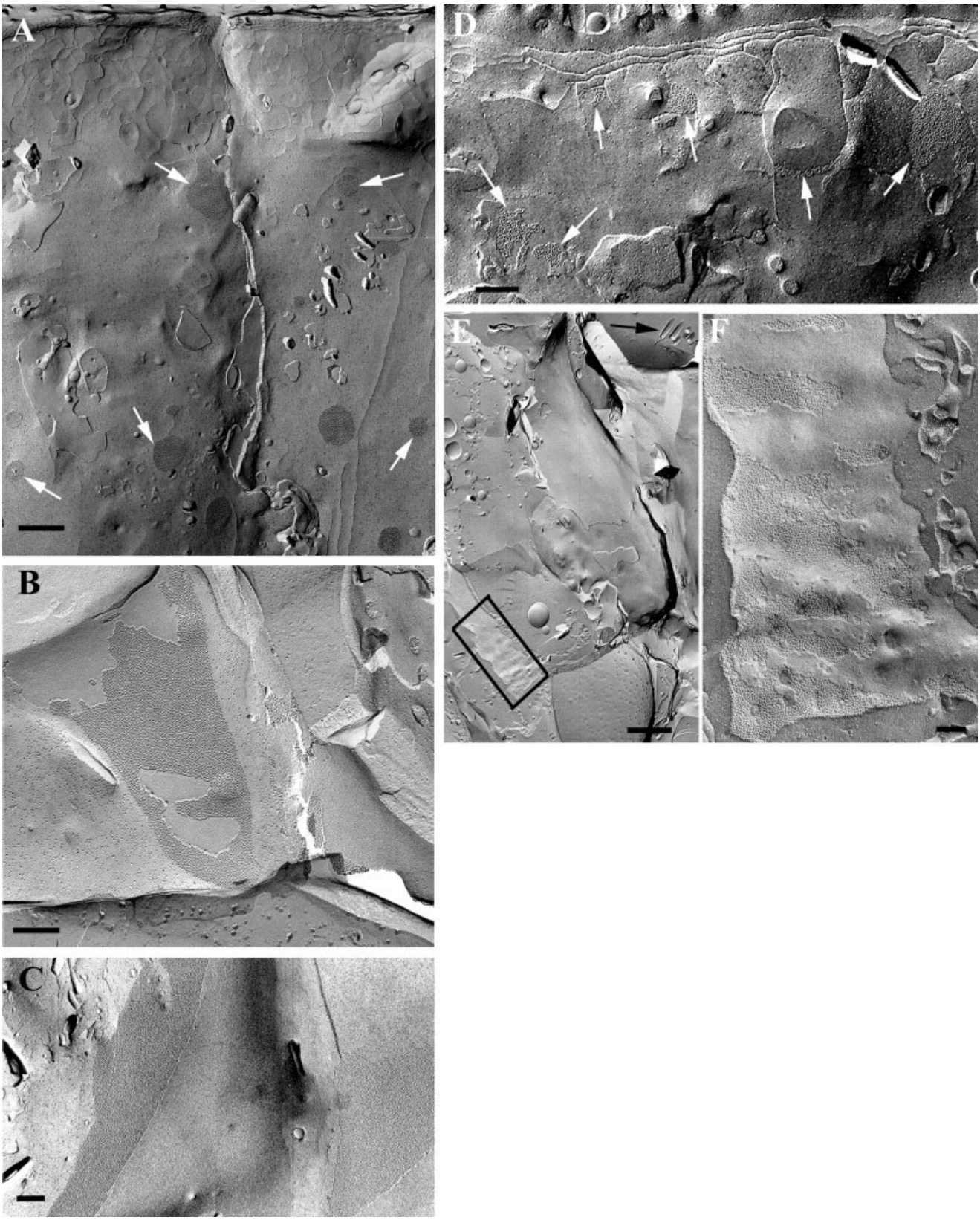

Figure 1

around the cell body of avian supporting cells were extremely large, some more than 4 μm^2 in area, i.e., with more than 50,000 channels (Fig. 1C).

The distribution and relative sizes of gap junction plaques were essentially the same in the basilar papillae of geckos and birds. Smaller junctions were present toward the lumenal side of the epithelium (Fig. 1D), with very large junctions more basally (Fig. 1E,F). Many of these junctional plaques around the cell body region of basilar papilla supporting cells were enormous, containing more than 100,000 channels (8 μm^2), often so large that in many cases the plaque covered the entire exposed membrane face and clearly extended beyond it (Fig. 1F), making estimation of the actual size impossible.

In the organ of Corti, the distribution of gap junction plaques and their relative sizes conformed generally to the pattern in the other sensory epithelia. Plaques were present where supporting cell heads contact each other at the lumenal side and also were present around the cell bodies. Those between the heads of Deiters cells were usually small, often with fewer than 100 connexons (Fig. 2A), but some were much larger, with about 10,000 channels. (Fractures exposing membranes in this region of Deiters cells were quite rare, limiting our ability to make a comprehensive analysis.) Between the bodies of adjacent Deiters cells, junctions were numerous, ~125/100 μm^2 of membrane, and often quite large (mean 2,000 channels/plaque, nominal channel density ~2,500/μm^2 of plasma membrane; Fig. 2B). The plaques between the body of the outer pillar cell and that of the first row of Deiters cells were similar to those between adjacent Deiters cells. The inner pillar cells provided an extreme example of the differential size distribution between basal and lumenal ends of the supporting cells. At the lumenal side, over the plasma membrane contact between the inner and the outer pillar cells, numerous very small plaques were present (Fig. 2C). These had a mean size of ~46 channels/plaque and were present at a density of ~800 plaques/100 μm^2 (nominal channel density ~370/μm^2 of plasma membrane). Potentially, they would provide communication pathways in the radial direction across the organ of Corti. In contrast, in the cell body region, the plaques were enormous, often appearing to occupy almost the entire membrane face in the regions of contact between adjacent inner pillar cell bodies (Fig. 2D). These junctions contained over 100,000 channels in most cases and potentially would provide communication pathways in the longitudinal direction along the organ of Corti. All down the region of contact between the inner pillar cell and the inner phalangeal cell were large numbers of small gap junction plaques, of a similar size and density to those between the inner and outer pillar cells (not shown). These junctions, again, would provide communication in the radial direction. Gap junction plaques were also large and ubiquitous on the cells to the inside and outside of the organ of Corti strip. To the inside, individual junctional plaques on the inner border cells and of the inner sulcus (see Fig. 9A) and, to the outside, those of Hensen cells and Claudius cells ranged in size up to ~3 μm^2 (37,500 channels), and gap junction plaques sometimes occupied in total over 25% of the total plasma membrane area in cells in these regions.

Mammalian cochlear lateral wall. In the lateral wall of the mammalian cochlea, gap junction plaques were numerous between fibrocytes in the spiral ligament and associated with the plasma membrane of basal cells in the stria vascularis (Forge, 1984; Souter and Forge, 1998). Those on the plasma membranes of fibrocytes (Fig. 3A,B) below the stria vascularis and those between fibrocytes and strial basal cells may contain up to ~30,000 channels (mean 2,892). Within an individual contact area between adjacent cells, there may be more than 20 separate junctional plaques (Fig. 3A). On the plasma membranes between adjacent basal cells, plaques were generally confined between the strands of the tight-junctional complexes (Forge, 1984; Souter and Forge, 1998; Fig. 3C). Analysis of these junctions in mice revealed a density of ~8 plaques/μm^2, and, although many of these were quite small (mean ~330 channels), they could range in size to over 8,000 channels/plaque. On the membrane of the basal cell that faces inward toward the body of the stria in mice (Fig. 3D), plaques of a size between about 20 and 6,000 channels (mean 878 channels, median 390) were present at a density of ~160/100 μm^2 of the total plasma membrane area exposed. Similar plaque sizes and densities were found on the equivalent membrane face in guinea pigs and gerbils (Forge, 1984; Souter and Forge, 1998). In bats, gap junction plaques on the strial-facing membrane of basal cells were present at much higher density (Fig 3E), a mean density of 6/μm^2 of exposed membrane face, with sometimes as many as 11/μm^2, and occupying in total as much as 44% of the exposed membrane area, but they were generally much smaller than in mice, guinea pigs, and gerbils, never containing more than 2,500 channels and with a mean size of ~250 channels (median 182). These junctions appeared to be formed between basal cells and intermediate cells. Gap junction plaques were not present on identifiable marginal cell basal processes at points of contact with basal cell membranes. As described previously for guinea pigs (Forge, 1984) and gerbils (Souter and Forge, 1998), there were no gap junction plaques on the membranes around the cell body region of marginal cells, where adjacent marginal cells appose each other, in either mice or bats.

Connexins expressed in the mature mammalian inner ear

RT-PCR was used to screen mature cochlear and vestibular tissues for 10 different connexins. This revealed

Fig. 1. Freeze-fracture replicas of supporting cell membranes in the utricular maculae of guinea pig (A,B) and owl (C) and the basilar papilla of chicken (D) and owl (E,F). Gap junction plaques are revealed as distinct clusters of particles. **A:** Numerous relatively small plaques (arrows) are present below the region of tight junction strands at the lumenal end of the supporting cells in the guinea pig utricular macula. **B:** Large plaque on membrane of cell body region in guinea pig utricular macula. **C:** Part of the fracture faces of the membranes in the cell body region of a supporting cell in owl utricular macula. The entire exposed fracture faces show the p-face particles or e-face pits of a single gap junction plaque. Scale bar = 0.2 μm in B,C,D. **D:** Membrane fracture face of lumenal end of supporting cell in chicken basilar papilla also shows numerous relatively small plaques (arrows) below the region of the tight junction. **E:** Low-power view of owl basilar papilla for orientation. Arrow indicates the hair bundle of hair cell. The boxed area, around the region of membrane of the supporting cell, is shown at higher power in F. **F:** Large gap junction plaque on membrane of supporting cell body region of owl basilar papilla, in the area enclosed by the box in E. Scale bars = 0.5 μm in A; 0.2 μm in B–D,F; 2 μm in E.

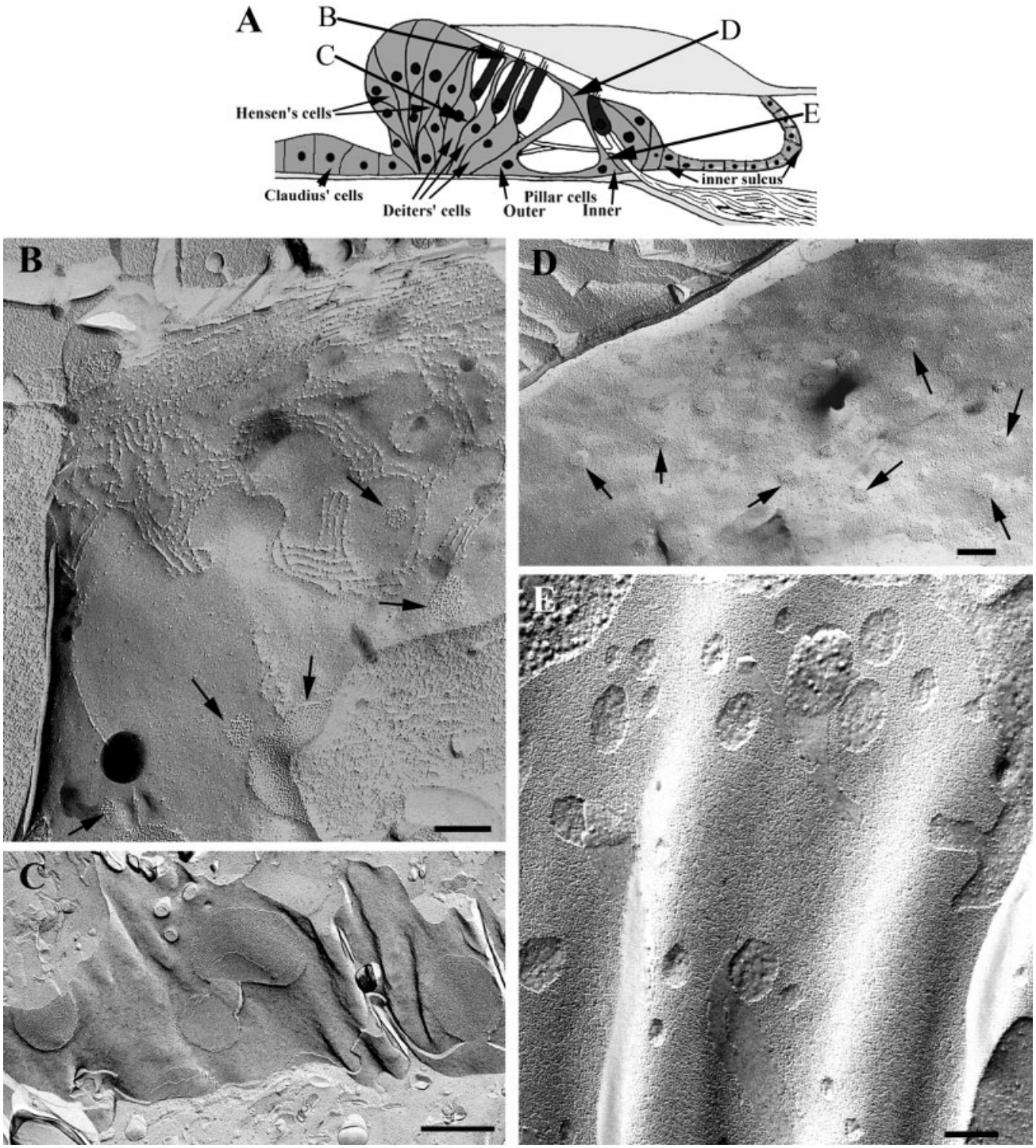

Fig. 2. Freeze-fracture replicas of supporting cells in the organ of Corti. **A:** Diagram of the organ of Corti, indicating location of membrane facture faces shown in B–E. **B:** Apical end of Deiters cell (mouse). Several small gap junction plaques (arrows) below the tight junction. **C:** Cell body region of Deiters cell (guinea pig). Several closely spaced larger plaques. **D:** Apical end of inner pillar cell at point of apposition with head of the outer pillar cell in mouse cochlea. Numerous very small plaques (arrows). **E:** Region of apposition between cell bodies of adjacent inner pillar cells (guinea pig). The entire membrane face shown is part of a single gap junction plaque. Scale bars = 0.2 μm.

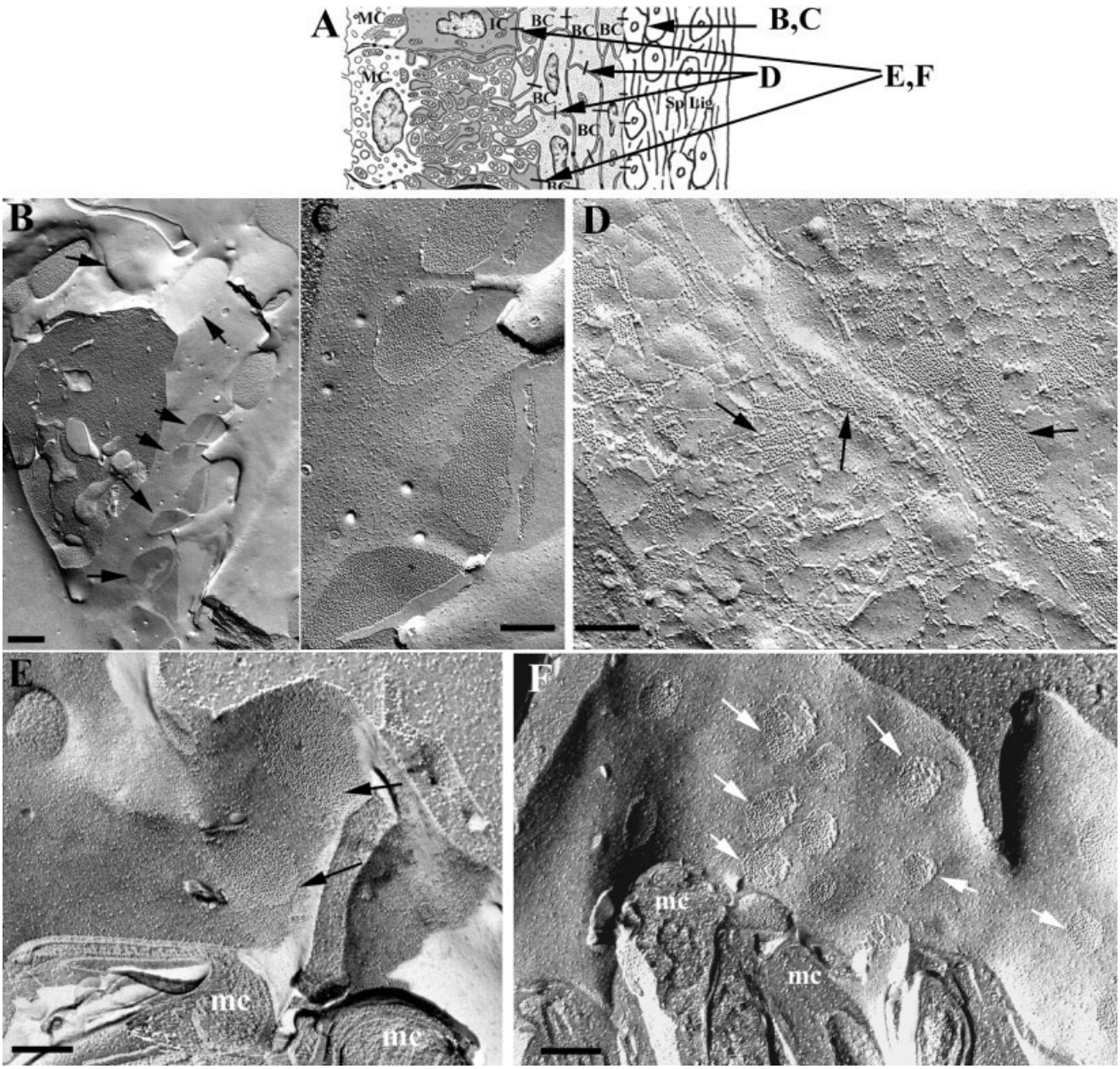

Fig. 3. Freeze-fracture replicas of spiral ligament fibrocytes and basal cells of the stria vascularis. **A:** Diagram indicating locations of membrane fracture faces shown in B–F; MC, marginal cell; IC, intermediate cell; BC, basal cell. **B:** Low-power view of ligament fibrocyte in mouse in region just below basal cells of the stria vascularis showing large number of plaques on the membrane of a single cell (arrows). **C:** Higher power view of part of membrane of cell in A to show size of plaques. **D:** Membrane faces at apposition between adjacent basal cells in stria vascularis of mouse. Gap junction plaques of various sizes and shapes (arrows) are present in the islands between tight junction strands. **E:** Basal cell membrane facing stria vascularis in mouse. Several junctions are evident (arrows), but plaques are not present at the point of apposition between marginal cell processes (mc) and the basal cell membrane. Marginal cell process is identified by the large mitochondrion, characteristic of marginal cells, that it encloses which is exposed on cross-fracture. **F:** Basal cell membrane facing stria in bat. Gap junction plaques (arrows) are more numerous and smaller than on the equivalent membrane fracture faces in mice (D), but again there are no plaques where the marginal cell processes (mc) appose the basal cell membrane. Scale bars = 0.5 μm in B; 0.2 μm C–F.

the presence of mRNA for cx26, cx30, cx31, cx43, and cx50 (Fig. 4A,B). However, mRNA for cx32 was not detected in either the cochlea or the vestibular system (Fig. 4A), nor were any of the other connexin mRNAs for which we screened (cx30.3, cx37, cx45, cx47). Western blotting (Fig. 4C) confirmed the presence of the cx26, cx30, and cx43, and a single faint band indicating a protein of approximate molecular weight of 50 kD was revealed with the antibody to cx50. However, in line with the PCR results, cx32 protein was not detected in protein extracts of the

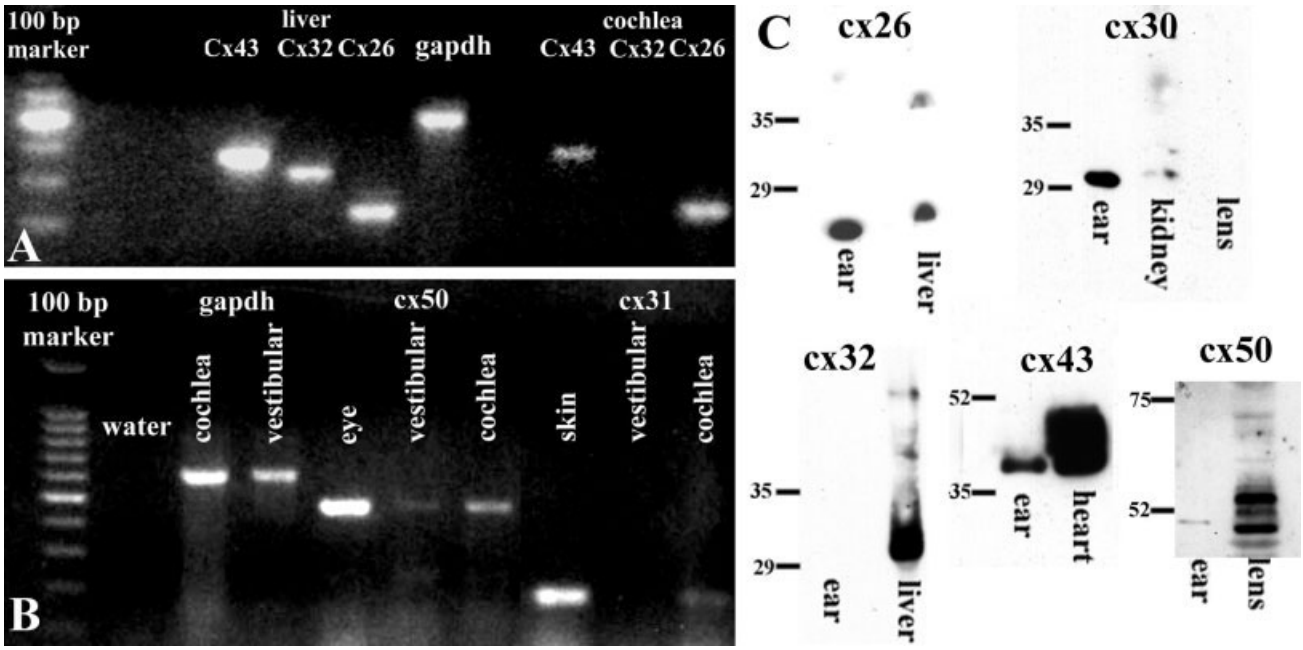

Fig. 4. RT-PCR (**A,B**) and Western blots (**C**) to identify connexins in preparations of the inner ear. Neither cx32 mRNA transcripts nor the protein is detected. Cx31 transcripts are present in the cochlea but are absent from preparations of the vestibular system.

inner ear (Fig. 4C), nor were the other connexin proteins, cx45 or cx46, for which we tested (not shown).

Immunohistochemistry

Positive immunoreactivity in the mature inner ear was detected for four connexins, cx26, cx30, cx31, and cx43. Antibodies to cx26 and to cx30 labeled in the vestibular sensory epithelia and throughout the organ of Corti, as well as at the basal limit of the stria vascularis and among fibrocytes in the spiral ligament. Labelling for cx31 and for cx43 was more restricted.

In vestibular sensory epithelia of mice, gerbils, and guinea pigs, antibodies to cx26 (Fig. 5A) and cx30 (Fig. 5B) both labeled large puncta at the basal aspects of the epithelium and smaller puncta more lumenally. In whole-mount preparations, tissue labeled with either cx26 (Fig. 5C) or cx30 (Fig. 5D) showed puncta surrounding the cell borders with no obvious asymmetry in distribution, indicating the likelihood of gap junctions connecting every supporting cell to each of its neighbours. There was also evidence for punctate cx43 immunoreactivity toward the basal limit of the sensory epithelia (Fig. 5E). Cx43 labeling was pronounced in the nonsensory tissues lining the vestibular compartments.

Neither cx31 nor cx43 could be detected in the organ of Corti, but antibodies to cx26 and to cx30 both labeled it intensely (Fig. 6A–F). The patterns of labeling for these two connexins coincided, and frozen sections doubly labeled with a polyclonal antibody to cx26 (Fig. 6B) and a monoclonal to cx30 (Fig. 6F) suggested the two connexins to be colocalised. Numerous large puncta were labeled intensely in the inner sulcus and the supporting cells surrounding the inner hair cells. In whole-mount preparations, in the region of the pillar cells (Fig. 6A,C), lines of labeling crossed the space between the regions of the inner and the outer hair cells, suggesting the presence of connexins within large gap junctions that would connect cells longitudinally along the organ of Corti. Individual confocal optical section images of whole-mount preparations stained with phalloidin (Fig. 6C) showed these junctions at the level of the actin bundles within the pillar cell bodies. In frozen sections, the cell body region of the inner pillar cell was intensely labeled (Fig. 6B,F), but the labeling in this region of the outer pillar cell, though intense, was less extensive. In the region of outer hair cells, labeling for cx26 and for cx30 was present around the cell bodies of Deiters cells (Fig. 6B,F) at the level of the actin bundles at the base of the cell (Fig. 6D,E), and puncta were present up the cell bodies of all the Deiters cells to a level just below the bottom of the hair cells (Fig. 6B,E,F). The labeled puncta surrounded individual Deiters cell bodies, suggesting the formation of gap junctions in both radial and longitudinal directions and that each Deiters cell is coupled to all its neighbours (Fig. 6A,D,E). Labelling was also present distinctly along the border between the Deiters and outer pillar cell (Fig. 6C) in a pattern suggesting radial coupling between these cell types. Both cx26 and cx30 labeling also delimited the circumferences of the Hensen, Claudius, and Boetcher cells to the outside of the organ of Corti (Fig. 6A,E).

In the lateral wall of the cochlea, fibrocytes beneath the stria vascularis were labeled with both cx26 and cx30 antibodies (Fig. 6G,I). Positive immunoreactivity for both connexins was also evident among basal cells of the stria vascularis (Fig. 6H,J). With cx30, in particular, the labeling clearly outlined the anatomical extent of the basal cell layer, with labeling extending into the apicalward basal cell extensions (Fig. 6J). However, there was no labeling

for either connexin at the level of the marginal cell bodies. Double labeling for cx26 and cx30 confirmed colocalisation of the two connexins among fibrocytes beneath the stria vascularis and in the basal cell region (Fig. 6K) but also revealed that labeling for cx30 was essentially absent and that that for cx26 was apparently much reduced, in the subpopulation of ligament type 2 fibrocytes below the spiral prominence.

Cx31 was detected among fibrocytes in ethanol-fixed tissue of mouse cochlea labeled with the anti-mouse cx31 antibodies and in paraformaldehyde-fixed guinea pig tissue labeled with the anti-human cx31 antibody. The labeling was confined to a distinct subregion of the ligament below the spiral prominence (Fig. 6L) that approximately coincided with that where labeling for cx30 and cx26 was low or absent. Cx31 was absent from the fibrocytes directly beneath the middle and upper region of the strial length and was not evident in the basal cell layer of the stria vascularis (Fig. 6L). Cx43 labeling in the cochlea was obtained with the commercial antibody from Chemicon but was confined only to cells lining the inside of the bony wall and into a pyramidal projection toward the basilar membrane (Fig. 6M). It was not evident in the stria vascularis nor the ligament fibrocytes beneath the stria.

Specificity of cx26 and cx30 antibodies

The labeling patterns with antibodies to cx26 and cx30 suggest that both connexins may be present in the same gap junction plaques, but cx26 and cx30 share significant sequence similarity, especially in the cytoplasmic loop, the region containing the epitope to which the antibodies to cx26 were raised. In Western blots of preparations of inner ear tissue, the monoclonal antibody to cx26 labeled only a single band at a position consistent with that of a protein of molecular weight ~26 kDa (Fig. 4C). Likewise the antibody to cx30 labeled only a single band at a position consistent with that of a protein of molecular weight ~30 kDa (Fig. 4C). To ensure the specificity of antibodies in immunohistochemical labeling, HeLa cells, which have no endogenous connexin expression, were transfected with cDNA of either cx26 or cx30 together with cDNA for green fluorescent protein to label transfected cells. Subsequent immunolabeling of cells transfected with cDNA for cx30 revealed labeled puncta at points of contact between adjacent cells only with the cx30 antibody and not the polyclonal cx26 antibody. Cells transfected with cDNA for cx26 showed labeled puncta only with the polyclonal antibody

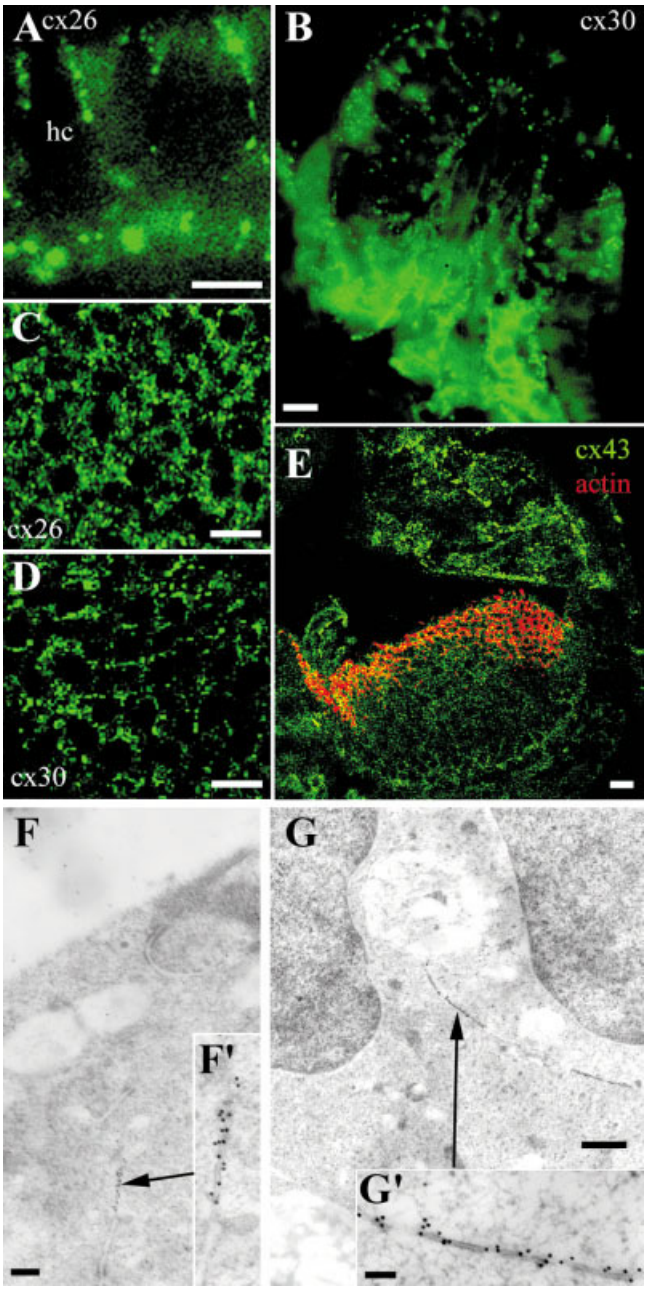

Fig. 5. Vestibular sensory epithelia of mouse labeled for connexins by immunohistochemistry (A–E), and of guinea pig by immunogold labeling (F,G). **A:** Frozen section of utricular macula labeled for cx26 imaged with standard epifluorescence. Labelled plaques are present between cells at the lumenal side and larger ones in the region of the supporting cell bodies. Hair cells (hc) are evident as unlabeled shapes. **B:** Frozen section of crista labeled for cx30 imaged by standard epifluorescence. Labelled plaques are present between cells toward the lumen and in the basal region between the bodies of supporting cells. Cx30 is also present in gap junction plaques in the connective tissue underlying the sensory epithelium. **C,D:** Single confocal optical sections of whole mounts of utricular macula, viewed looking downward on the apical surface, labeled for cx26 (C) and cx30 (D). Punctate labeling at cell borders shows that plaques are more or less evenly distributed around the supporting cells. **E:** Confocal projection of frozen section of utricular macula labeled for cx43 (green) and with TRITC-conjugated phalloidin (red) to label actin at the apical surface of the sensory epithelium. Punctate positive immunoreactivity for cx43 in the sensory epithelium particularly toward the basal aspect in the region of supporting cell bodies. Cx43-positive labeling is also evident in cells lining the vestibular compartment. **F,F′:** Immunogold labeling with polyclonal antibody to cx26 in thin section of utricular macula. Arrow indicates gold particle labeling exclusively confined to the region of cell–cell contact toward the lumenal side of the epithelium that is shown at higher power in F′. The decorated membrane profile has a morphology consistent with that of a gap junction, and the gold particles are distributed evenly along and on both sides of the junction. **G,G′:** Immunogold labeling with polyclonal antibody to cx30 in thin section of utricular macula. Profile of large junction between the cell bodies of two supporting cells; arrow indicates the region in G of the image in G′. Gold particles are confined to the junction profile and decorate all along it and on both sides. Scale bars = 10 μm in A–E; 0.5 μm in F,G; 100 nm in F′,G′.

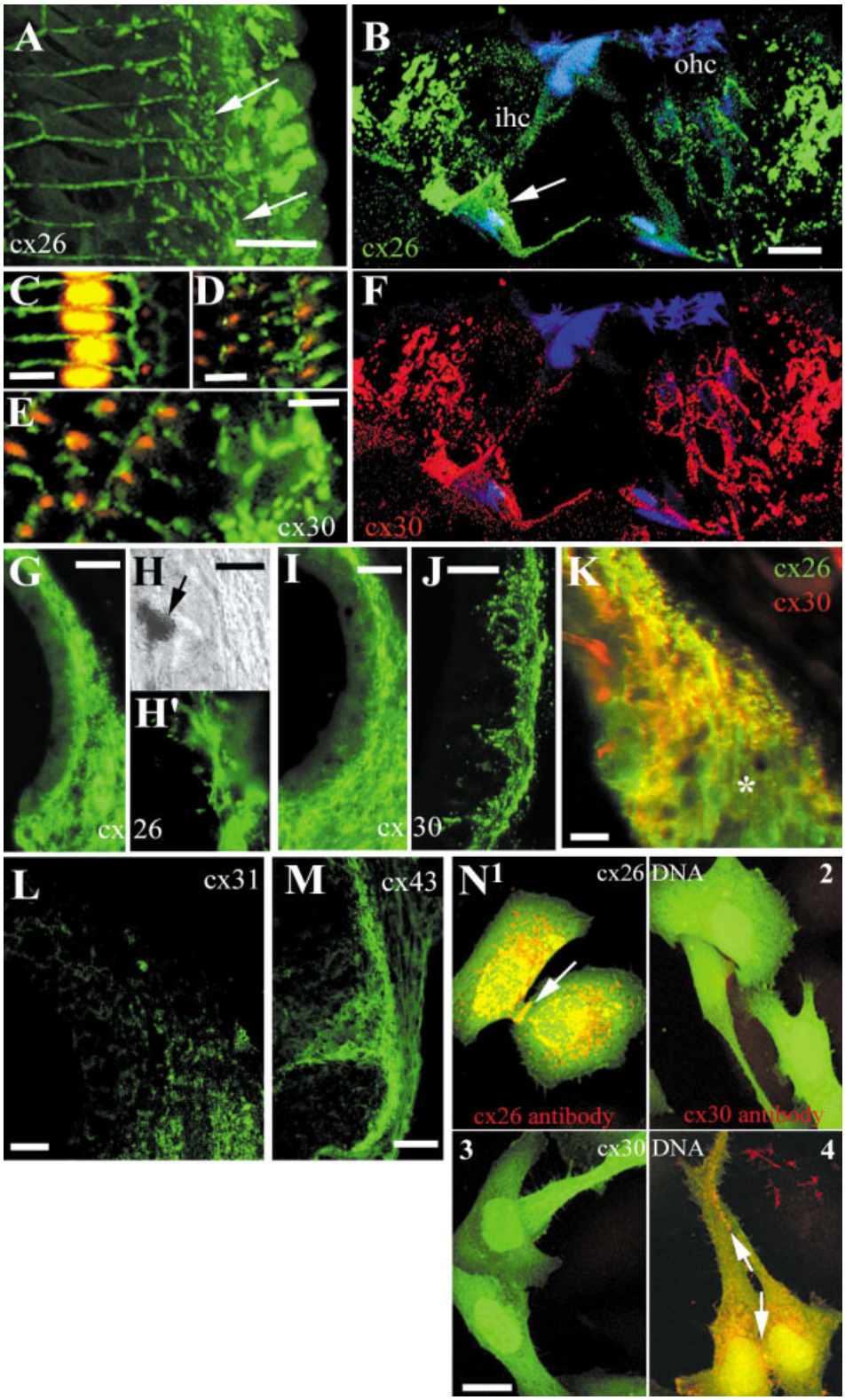
A
cx26
B
ohc
ihc
cx26
C
D
E
cx30
F
cx30
G
cx 26
H
H'
I
cx 30
J
K
cx26
cx30
*
L
cx31
M
cx43
N1
cx26
DNA
2
cx26 antibody
cx30 antibody
3
cx30
DNA
4

Figure 6

to cx26 and not with the polyclonal cx30 antibody (Fig. 6N).

Immunogold labeling of gap junctions

To determine the possible colocalisation of cx26 and cx30, those antibodies that had been tested for their specificity were used for immunogold labeling of thin sections of mouse or guinea pig inner ear tissues. All three of the antibodies (polyclonal to cx30, polyclonal to cx26, and monoclonal to cx26) labeled only along plasma membranes at sites with a morphology consistent with that of gap junctions, where membranes of two adjacent cells were in close apposition, but not at plasma membrane regions outside these points of contact (Figs. 5F,G, 7A–C). The intensity of gold particle labeling was high with the polyclonal antibody to cx26 (Figs. 5F, 7A) and the polyclonal cx30 (Figs. 5G, 7B) antibodies but was lower with the monoclonal antibody to cx26 (Fig. 7C); however, with all three antibodies, gold particles were present on both sides of individual junction profiles and evenly distributed along them.

Each of the antibodies labeled gap junction section profiles in every cell type across the organ of Corti, in the spiral ligament, among strial basal cells, and in the vestibular sensory epithelia. This suggested that gap junctions in these locations were composed of both cx26 and cx30. Double labeling of the same junction plaques confirmed the presence of both cx26 and cx30, and both connexins were evenly distributed on both sides of the junction. Stereo-pair imaging of mouse cochlear sections in which one surface had been exposed to anti-cx26 antibody and the opposite surface to anti-cx30 antibody showed that gold particles of the smaller size to detect one of the two antibodies was localised to one face all along and on both sides of the junction profile, and the larger gold particles used to localise the other antibody were confined to the opposite face and were also all along and on both sides of the junction profile (Fig. 7D). Likewise, where the same junction was sectioned in successive sections, it was labeled essentially identically in the section labeled for cx26 and in that labeled with cx30 antibodies (Figs. 7A,B, 8A,B). Gold particles were evenly distributed all along the junction profile with both connexin antibodies. Although the gold particles along much of the membrane profile appeared to be localised on one side of the junction (i.e., one cell rather than the other), they were on the same side for both of the connexins and at the sites where the gap junction was cross-sectioned the gold particles were evident on both sides of the junction (i.e., in both cells) both with cx26 antibody and with cx30 antibody (Fig. 8A,B). [The apparent asymmetry in the labeling is an artefact arising because the membrane is cut at an angle to the perpendicular, so only one side of the junction is exposed for antibody labeling. The opposite side is "buried" within the embedding plastic, which the aqueous labeling solutions do not penetrate. Only proteins exposed at the section surface can be labelled. This artefact can be resolved in the stereo-pair images (Fig. 7D), where, if one member of the pair is viewed alone, it appears that the small gold particles are on one side of the junction and the larger particles on the other, but the stereo imaging reveals that

Fig. 6. Immunohistochemical localisation of connexins in the mouse cochlea (A-M) and in transfected HeLa cells (N). **A:** Cx26 in organ of Corti whole mount viewed looking downward on the apical surface (i.e., perpendicular to diagram in Fig. 2A but of opposite orientation); confocal projection. Labeling in pillar cell region defines apparently large plaques between cells in the longitudinal direction along the organ of Corti. Arrow indicates puncta surrounding bodies of Deiters cells (level of C in Fig. 2). Hensen cells (at edge to the right) also show extensive labeling surrounding the cell bodies. **B:** Confocal image of frozen section of organ of Corti cut radially (i.e., similar to diagram in Fig. 2A but of opposite orientation) double labeled with polyclonal antibody to cx26 (green) and with phalloidin for actin (blue). Same section as that shown in F (cx30 labeling). Numerous puncta label for cx26 in the cell body region of Deiters cells below the outer hair cells (ohc). Intense labeling of the body region of inner pillar cell (arrow). There is also evidence of diffuse cytoplasmic labeling in the phalangeal process of the pillar cells. Punctate labeling of junctions in the region of Hensen cells to the outside (right of image) of cell borders of supporting cells around inner hair cell (ihc) and in the inner sulcus (to the inside, left). The section angle has cut through the apical end of one ihc, whose stereocilia and cuticular plate are evident (blue) and the cell body of the next adjacent ihc (indicated by *ihc*) with labeling for connexins in the region of the supporting cells between the two ihcs. **C–E:** Cx30 in organ of Corti whole mount. Single optical sections of the same preparation at different levels of focus (around region C in Fig. 2A); cx30 labeling in green and for actin with phalloidin in red. Pattern of labeling identical with that for cx26. C: Region of pillar cells at the level of actin bundles at the base of the cells. Labelling is all along cell borders in the radial direction, i.e., between apposing pillar cells in the longitudinal direction; but labeling in the longitudinal direction, i.e., between cells meeting radially, at the point of apposition between the outer pillar cell and the first row of Deiters cells. D: Deiters cell region, at the level of actin bundles at the cell base. Labelling for gap junction plaques surround each cell body and plaques appear to be of similar size with all neighbours. E: Deiters cells, just below level of the base of the ohcs, and Hensen cells. Labelled puncta surround each Deiters cell body and each Hensen and Claudius cell. Labelled gap junction plaques in the Hensen and Claudius cells are very large. **F:** Cx30 labeling (red) with monoclonal antibody and actin with phalloidin (blue) in the same section as in B. Cx30 labeling coincides almost precisely with that of cx26. **G,H:** Cx26 in sections of the cochlear lateral wall. G: Low power showing labeling among spiral ligament fibrocytes and in the basal aspect of the stria. H: Nomarski DIC image and H′ epifluorescence image of the same region of the stria vascularis. Arrow in H indicates pigment in an intermediate cell. The labeling for cx26 is confined to the basal cell region and does not extend into the marginal cell layer. **I,J:** Cx30 in lateral wall. I: Cx30 is present in fibrocytes of the spiral ligament and the basal region of the stria. J: Confocal optical section of stria vascularis separated from the spiral ligament. Punctate Cx30 labeling outlines the borders of basal cell including their apicalward extensions. **K:** Double labeling for cx26 (polyclonal antibody; green) and cx30 (monoclonal antibody; red) in a section of lateral wall shows that the two connexins are colocalised at the base of the stria and in the ligament beneath it, but there is greatly reduced intensity of labeling for both antibodies among fibrocytes below the spiral prominence (asterisk). Strial capillaries are highlighted in red owing to reaction of anti-mouse secondary antibody with the serum within them. **L:** Cx31 labeling in section of cochlear lateral wall. Relatively weak labeling is confined to a region of fibrocytes below the spiral prominence corresponding to that where cx26 and cx30 (K) are reduced or absent. **M:** Cx43 labeling in the lateral wall is present in cells lining the otic capsule at the level of the scala media and into the scala tympani, with a cone of labeling toward the point of attachment of the basilar membrane. **N:** HeLa cells cotransfected with cDNA for GFP and with cDNA for either cx26 (1,2) or cx30 (3,4) and immunolocalisation for cx26 (1,3) or cx30 (2,4) proteins (red). GFP throughout the cytoplasm. Arrows indicate gap junction plaques. Cx26 polyclonal antibody reveals plaques only in cells transfected with cx26 cDNA (1), and cx30 polyclonal antibody reveals plaques only in cells expressing cx30 (3), demonstrating that these antibodies do not cross-react. Scale bars = 20 μm in A,B,J–L; 10 μm in C,D,H; 5 μm in E,N; 50 μm in G,I,M.

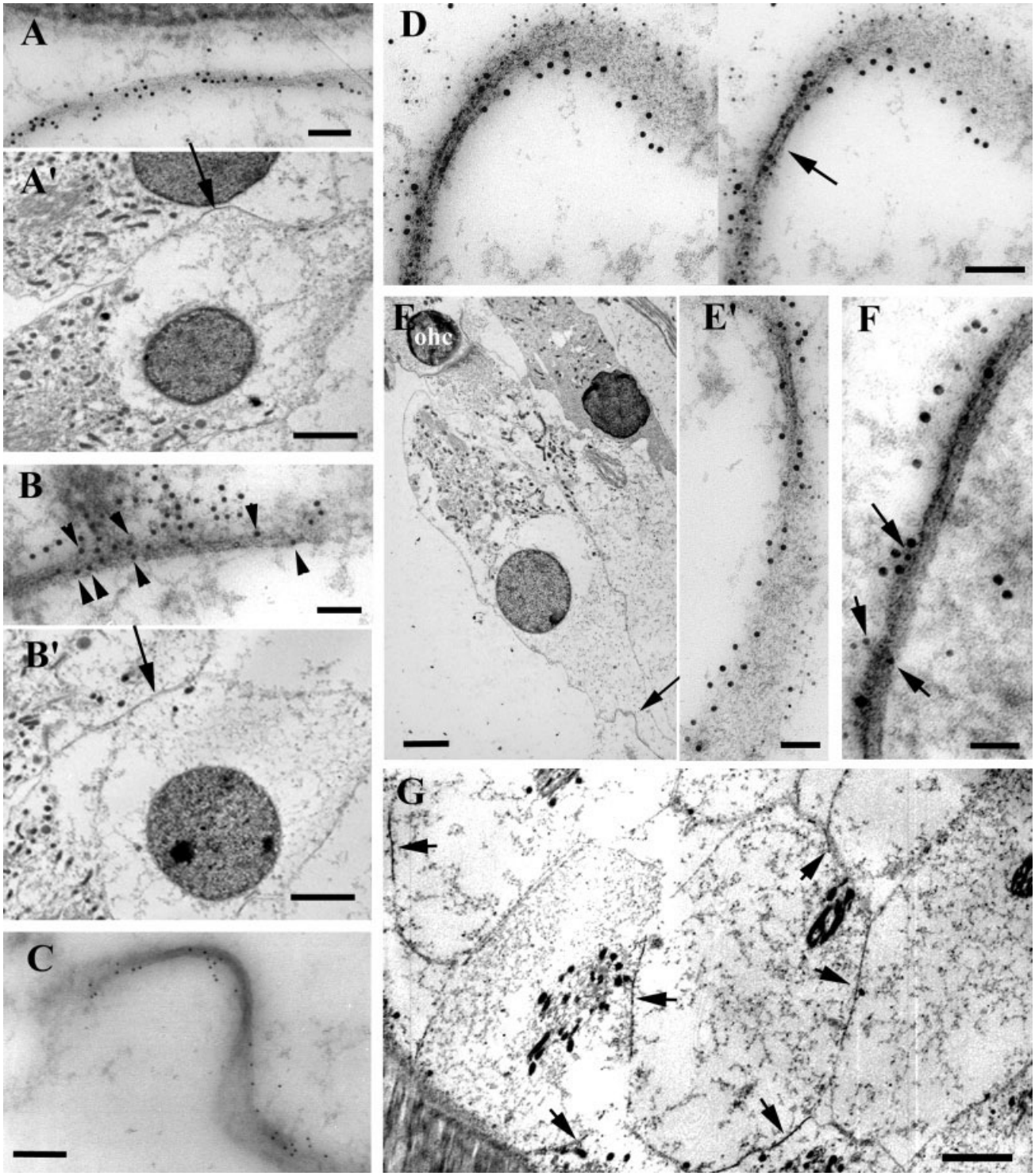

Fig. 7. Immunogold labeling of thin sections of Deiters cells. **A:** Cx26 polyclonal antibody. Gold particles (10 nm) label evenly along and both sides of the junction profile in a section of the mouse organ of Corti cut almost parallel to the basement membrane. The location of the junction is indicated by the arrow in **A′** showing that the junction is between cell bodies in the longitudinal direction along the organ of Corti (at approximately the level of C in Fig. 2A). **B:** Cx30 polyclonal antibody labeling (10-nm gold particles) of the same junction plaque in a section successive to that shown in A. Gold particles again are all along the junction profile and on both sides. Arrowheads denote location of gold particles either side of the junction profile. Arrow in **B′** shows the location of the junction between the two cells. C: Cx26 monoclonal antibody labeling of junction in guinea pig organ of Corti. Gold particle (5 nm) labeling is less intense than with the polyclonal antibodies but is again all along and on both sides of the junction profile. **D:** Stereo pair of thin section of junction in mouse organ of Corti doubly labeled with cx26 polyclonal antibody localised with 5-nm gold particles on one face of the section and with cx30 polyclonal and 10-nm gold particles on the other face. Stereo imaging reveals that the 10-nm particles are confined to one face and 5-nm particles to the other, but both label evenly all along the junction profile and on both sides. This is particularly evident at the point where the junction is precisely cross cut (arrow). **E,E′:** Junction between Deiters cell bodies in the radial direction (arrow in E; approximately equivalent to point C in Fig. 2A) in mouse organ of Corti doubly labeled with polyclonal to cx26 localised with 5-nm gold particles and polyclonal cx30 localised with 10-nm gold particles on opposite faces shown in E′; only one image of the stereo pair is shown in E′. Both cx26 and cx30 antibodies label evenly along the junction profile and on both sides. **F:** Junction in section of guinea pig organ of Corti doubly labeled on the same face with polyclonal antibody to cx26 localised with 5-nm gold particles and monoclonal antibody to cx30 localised with 10-nm gold particles. Arrows point to some of the 5-nm gold particles (cx26) present among 10-nm particles (cx30) and on both sides of the junction profile. **G:** Cell bodies of Deiters cells in a section cut almost parallel to the apical surface. Decoration of junctions with gold particles, in this case using 10-nm particles localising cx30, reveals their locations, indicated by arrows, and sizes. Each Deiters cell forms gap junctions with all its neighbours. Scale bars = 50 nm in A–C,F; 2 μm in A′,B′,G; 100 nm in D,E′; 5 μm in E.

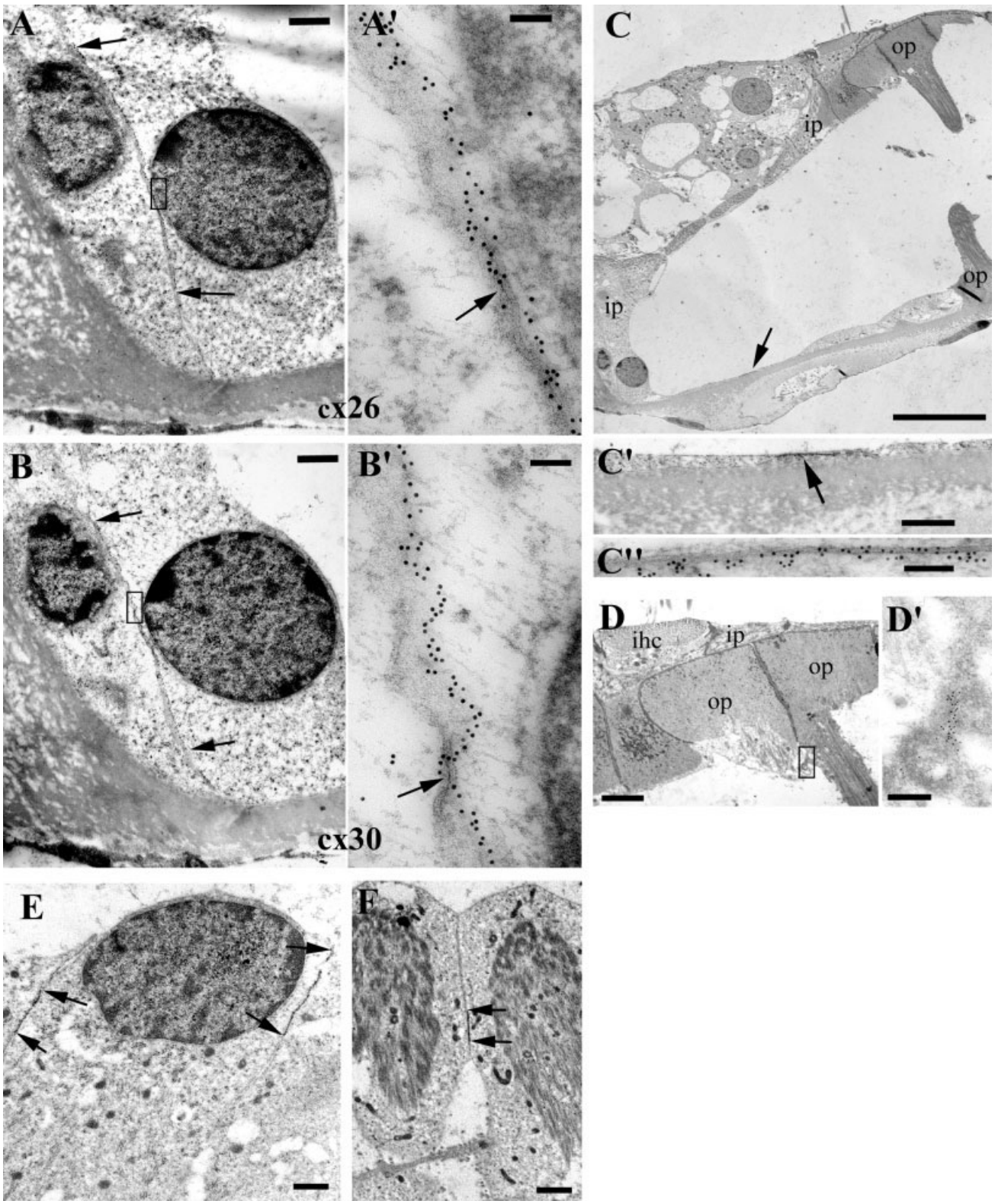

Fig. 8. Immunogold labeling of pillar cells. **A,B:** Successive sections of the same pair of apposing inner pillar cells (equivalent to E in Fig. 2) labeled for cx26 in A and for cx30 in B, each localised with 10-nm gold particles (mouse organ of Corti). The extent of the junction profile (~6 μm) is indicated by the arrows. The boxed areas are shown at higher power in A′,B′. With both cx26 and cx30, gold particles are evenly distributed all along the junction profiles. Arrows in A′ and B′ indicate where the junction is precisely cross-cut, and in each case particles are on both sides of the junction. **C:** Junction between feet of outer and inner pillar cells (op and ip, respectively) shown at successively higher magnifications to provide orientation in C, C′, and C′′ and labeled for cx30. The junction labels evenly for cx30 (C′′; the successive section, not shown, labeled evenly for cx26). **D:** Junction at apex between outer pillar cells (op; ip, inner pillar, ihc, inner hair cell) labeled for cx26 within the boxed area shown at higher power in **D′**. The junction links the cells in the longitudinal direction and labels evenly for cx26. Inner pillar cells (**E**) and outer pillar cells (**F**) in sections cut approximately parallel to the apical surface of the organ of Corti in guinea pig. Arrows indicate the limits of immunogold labeled junction profiles linking cells in the longitudinal direction. Junctions of inner pillar cells are much larger than those of outer pillar cells. Scale bars = 1 μm in A,B,C′; 100 nm in A′,B′,C′′; 10 μm in C; 2 μm in D–F; 0.2 μm in D′.

the particles of the different sizes are on opposite faces of the profile of a junction cut at an angle.]

The presence of cx26 and cx30 in the same gap junction plaques was also evident in guinea pig tissue labeled with the polyclonal anti-cx30 and monoclonal anti-cx26 (Fig. 7F), and again both antibodies labeled on both sides of junction profiles. However, in these double-labeled preparations, labeling for cx30 appeared to be much more extensive than that with the monoclonal for cx26 in all junctions examined, although this most likely is due to the relatively much greater efficiency of labeling with the polyclonal cx30 antibody in comparison with the monoclonal cx26 used for double labeling the guinea pig tissue. In both mouse and guinea pig, double labeling of individual junction plaques was evident among Deiters cells, between cells coupled longitudinally (Fig. 7A,B) and cells coupled radially (Fig. 7E); between the bodies of inner pillar cells in the longitudinal direction (Fig. 8A,B); between the inner and outer pillar cells at their apices and at their bases (Fig 8C); between outer pillar cells (Fig. 8D,F); in the region of Hensen cells; and in the inner sulcus and Claudius cells (Fig. 9).

The relative sizes of gold-labeled gap junction section profiles in the various cells coincided with those of gap junction plaques seen by freeze fracture, and the decoration of junctions provided by the intense gold particle labeling allowed their identification at relatively low magnification and, thus, an assessment of the distribution of junctions around each cell type. In vestibular organs, antibodies to cx26 and to cx30 labeled relatively short junction profiles between supporting cells toward the lumenal side of the epithelium and much longer profiles at junctions between the cell bodies (Fig. 5F,G). In the organ of Corti, within the inner sulcus and in Claudius cells, in sections cut parallel to the radial axis, several relatively long junction profiles were labeled in each cell (Fig. 9B), a pattern consistent with the large plaques seen by freeze fracture (Fig. 9A) and indicating radial coupling of cells in this region. In sections cut parallel to the apical surface, junctions were evident between cells in both the radial and the longitudinal directions, indicating that each cell is coupled to all its neighbours, and there was no obvious asymmetry between directions in the size of the junction plaques (Fig. 9C). A similar pattern was evident among Deiters cells in sections cut parallel to the apical surface: Each cell was coupled to all its neighbours in both the radial and the longitudinal directions (Fig. 7G). In the region of the bodies of inner pillar cells in sections cut radially across the organ of Corti, connexin antibody labeling extended for at least 6 μm along the plasma membrane profiles at points of close apposition between two adjacent cells (Fig. 8A,B), and, in sections cut parallel to the apical surface, similarly large junction profiles were exposed (Fig. 8E). The large size of the junction profiles in the cell body region of the inner pillar cell is consistent with the enormous gap junction plaques exposed on the membrane faces of inner pillar cells by freeze fracture. In sections approximately parallel to the long axis of the organ of Corti, membrane profiles labeled with both cx26 and cx30 were also evident between the heads of outer pillar cells at their apices (Fig. 8D) and between the bodies of the outer pillar cells (Fig. 8F), indicating, again, communication pathways in the longitudinal direction between these cells, but the sizes of the gap junction plaques between the bodies of outer pillar cells were generally smaller than those between inner pillar cells. Between the outer and the inner pillar cells in the head region, there were very short labeled profiles (not shown) consistent with the small gap junction plaques in this region, and membrane profiles that labeled with both cx26 and cx30 antibodies were present between the feet of the outer and inner pillar cells at the base of the tunnel Corti (Fig. 8C). The position of these junction profiles suggests radial communication between inner and outer pillar cells. Junction profiles between inner pillar cells and phalangeal cells also suggest potential radial communication between these cell types. Likewise, in the outer regions of the organ of Corti, sections cut radially and sections cut parallel to the apical surface indicated coupling of Hensen cells to each other in the longitudinal direction, to Deiters cells in the radial direction, and to all other neighbouring cells.

In the stria vascularis, there were junction profiles of a size consistent with the size of gap junction plaques as seen by freeze fracture that were doubled labeled for cx26 and cx30 between basal and intermediate cells (Fig. 10A), between adjacent basal cells (Fig. 10B), between basal cells and fibrocytes of the spiral ligament (Fig. 10C), and among fibrocytes in the spiral ligament (Fig. 10D). However, although gold-labeled junction profiles were clearly evident where basal cells apposed intermediate cells, gold particles were never observed on the membrane at the tips of the marginal cell basal projections (Fig. 10A), nor were gold particles evident on the lateral membranes of adjacent marginal cells or where marginal cells contacted intermediate cells.

Coimmunoprecipitation

The immunogold labeling suggested that cx26 and cx30 are both present and evenly distributed in individual gap junction plaques. To confirm that both can be present in the same connexons, immunoprecipitation of membrane proteins from mature mouse cochleae solubilised in DM, which preserves connexon oligomers (Stauffer et al., 1991), was performed. In the samples precipitated with antibody to cx30, both cx26 and cx30 were present (Fig. 11A). Likewise, both cx26 and cx30 were present in samples precipitated with cx26 antibodies (Fig. 11B). In samples of cochlear membranes solubilised with SDS, which destroys oligomeric structures, however, only cx30 was evident in the cx30 precipitate (Fig. 11A) and only cx26 in the cx26 precipitate (not shown).

Annular gap junctions

In thin sections of conventionally prepared, unlabeled tissue, some cells often contained intracellular vesicles, with double membranes, sometimes splitting apart, with a morphology similar to that of gap junction profiles (Fig. 12A). In freeze-fracture replicas, apparently intracellular gap junction plaques over a spherical membrane face were evident (Fig. 12B). In sections immunogold labeled for either cx26 or cx30, intracellular vesicles with membranes decorated evenly with gold particles were often present in many cells (Fig. 12C), and, in double-labeled sections, the membranes of these vesicles were labeled evenly and on both sides with both cx26 and cx30 (Fig. 12D) in a manner similar to that of gap junction plaques at the plasma membranes. Such vesicles appeared to arise by invagination of the plasma membrane and were often located quite close to the inner side of the plasma membrane (Fig. 12E). However, some were present close to the nucleus (Fig.

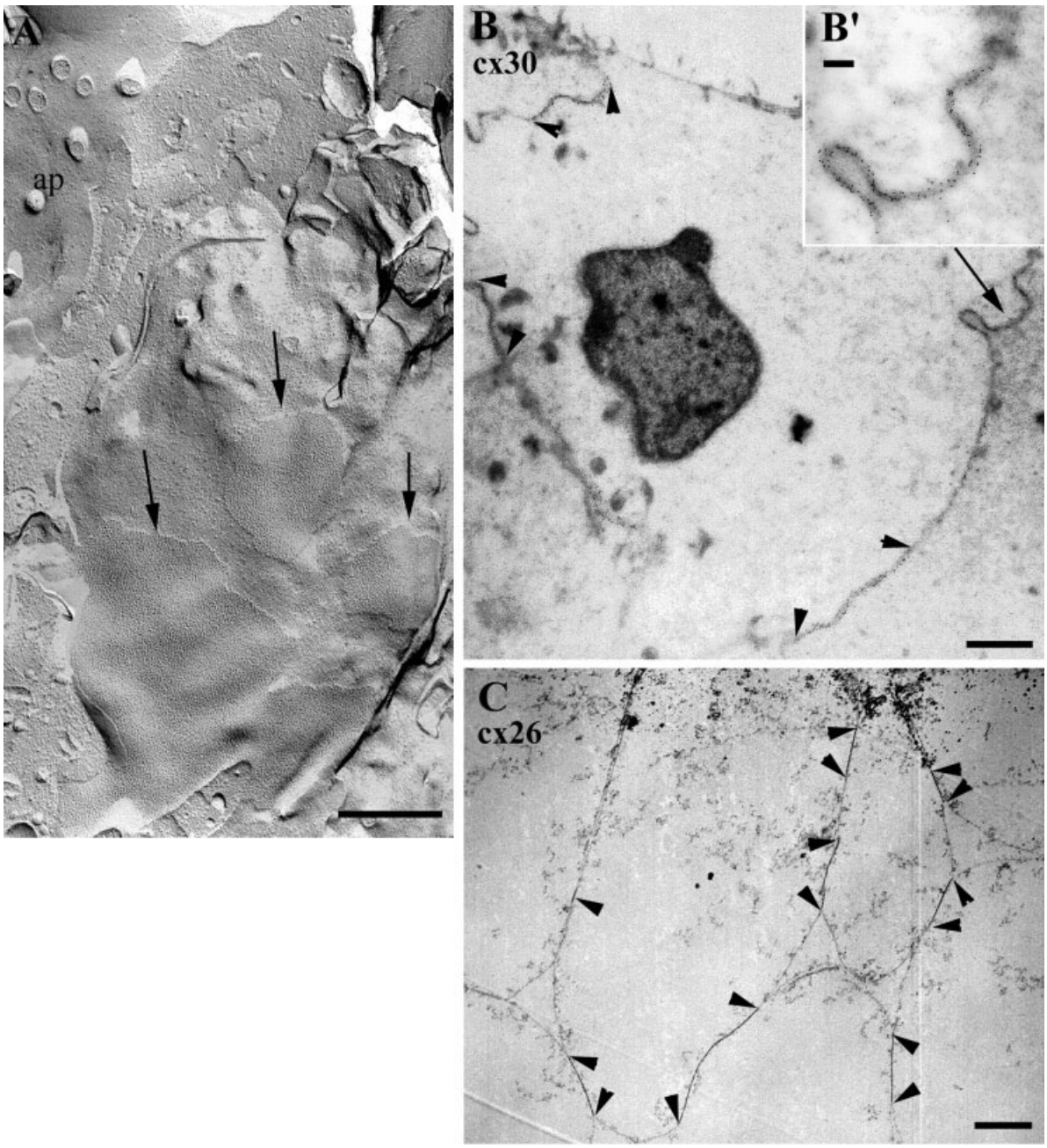

Fig. 9. Inner sulcus cells (A,B) and Claudius cells (C). **A:** Freeze fracture of guinea pig organ of Corti reveals several large plaques (arrows) covering a significant proportion of the membrane fracture face of an inner sulcus cell. **B:** Thin section of inner sulcus cell in guinea pig organ of Corti labeled for cx30. Arrowheads indicate limits of labeled gap junction profiles and arrow indicates the junction shown at higher power in **B′**. The sizes and distribution of the labeled junction profiles coincide with those of the plaques revealed by freeze fracture. The junctions label evenly for cx30 (B′). **C:** Section through Claudius cells in mouse cut parallel to the apical surface, and labeled for cx26, shows that each cell forms several large gap junctions with all its neighbours. Arrowheads indicate limits of gold particle-decorated junction profiles. Scale bars = 0.5 μm in A; 1.0 μm in B; 0.2 μm in B′; 2 μm in C.

12F), where they showed signs of degeneration (Fig. 12G). The characteristics of these membranes are consistent with those of annular gap junctions that are thought to be formed as part of the process of gap junction removal from the plasma membrane and indicate turnover of gap junctions in those cells in which they are present. In the organ of Corti, such labeled vesicles were particularly evident in cells of the inner sulcus and in Claudius and Hensen cells but were less evident in inner and outer pillar cells. They were also present in fibrocytes of the spiral ligament (Fig 12C) and in basal cells of the stria vascularis.

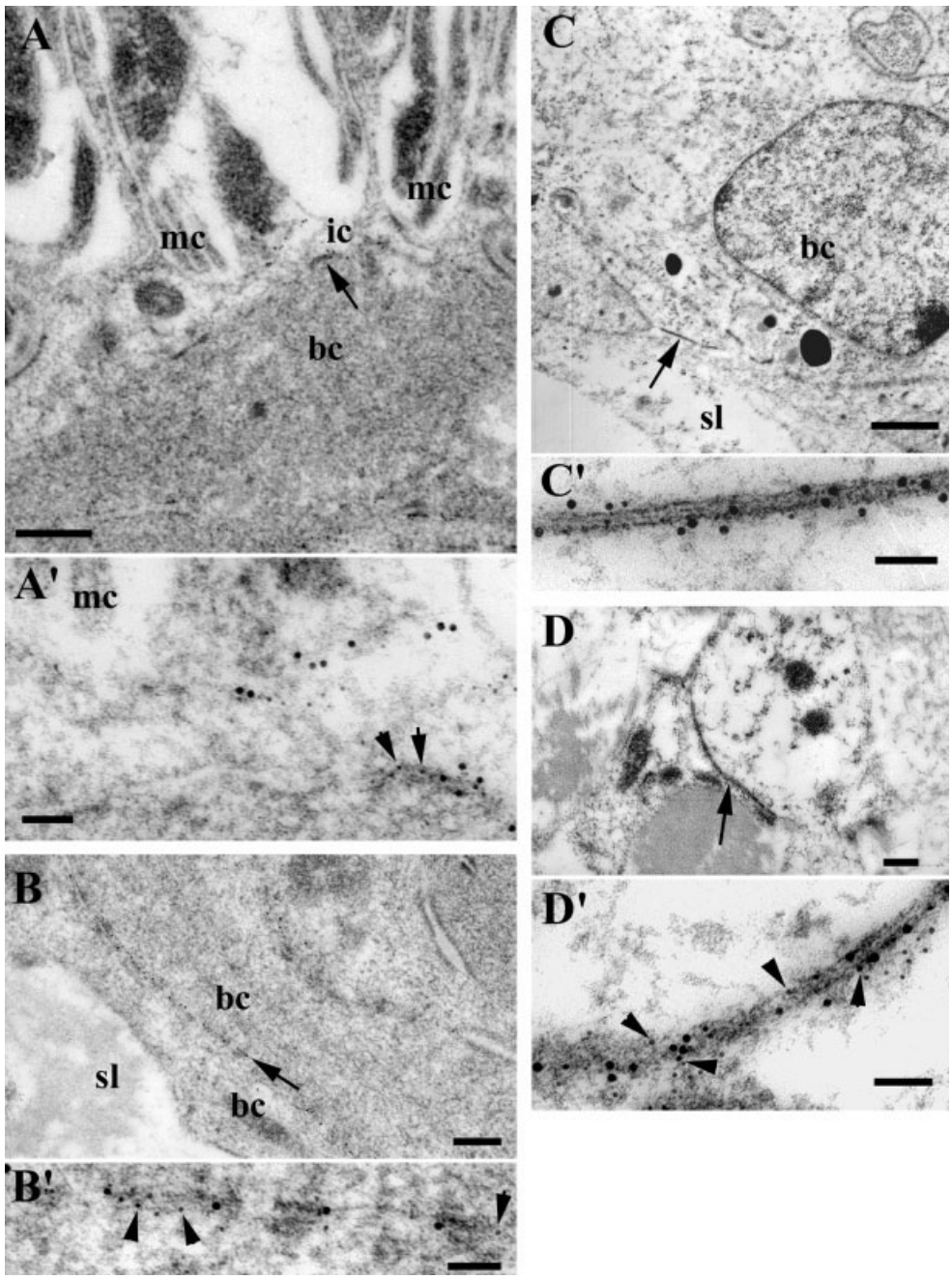

Fig. 10. Immunogold labeling of thin sections of stria vascularis and spiral ligament. **A:** Stria vascularis in mouse in region of apposition of basal cells (bc) with the marginal and intermediate cells (mc, ic; region E and F in Fig. 3) doubly labeled with polyclonal cx26 and polyclonal cx30 on opposite faces of the section. **A′** shows the junction arrowed in A, and both cx26 (5-nm gold particles, arrow in A′) and cx30 (10-nm gold particles) are evident on the same junction profile between a basal cell and an intermediate cell. There are no gold particles associated with the tip of the marginal cell process (mc) where it meets the basal cell. **B:** Junction between adjacent basal cells (bc) in mouse labeled as in A; sl, spiral ligament. The arrow indicates the junction shown in **B′**, which again is decorated with both 5-nm gold particles localising cx26 (arrowheads) and 10-nm particles localising cx30. **C:** Junction (arrow) between basal cell (bc) and fibrocyte in the spiral ligament (sl) in guinea pig doubly labeled with polyclonal to cx26 localised with 5-nm gold particles and monoclonal cx30 localised with 10-nm gold particles. **C′** shows both connexins evenly distributed along the junction profile. **D:** Junction between fibrocytes in the spiral ligament (arrow) in guinea pig labeled as in C. In **D′**, arrowheads indicate 5-nm particles, localising cx26, evenly distributed among larger gold particles localising cx30. Scale bars = 0.2 μm in A–C; 50 nm in A′–D′; 1 μm in D.

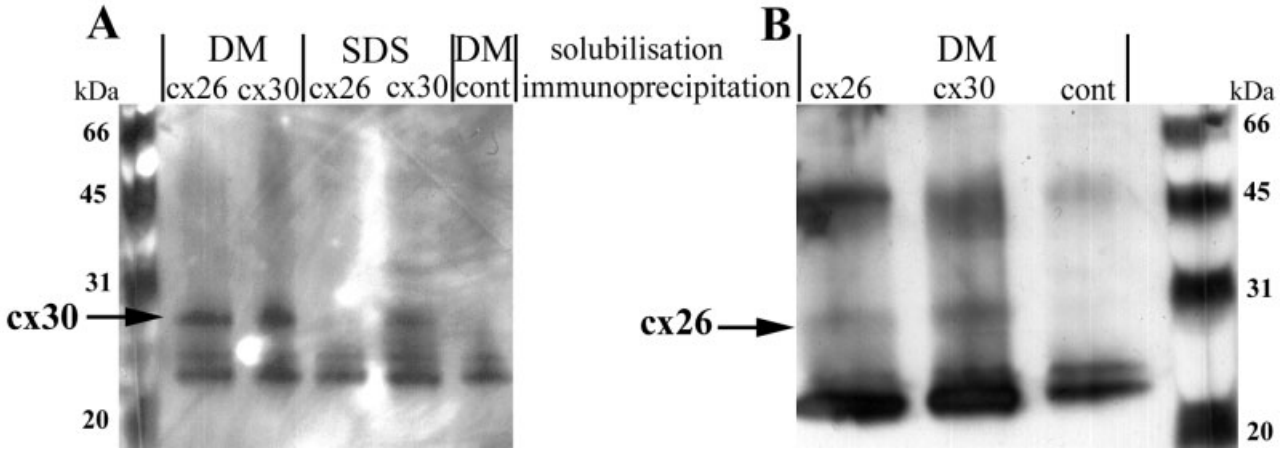

Fig. 11. Coimmunoprecipitation of cx26 and cx30. **A:** Western blot of separated membrane proteins solubilised with dodecyl maltoside (DM) or SDS and precipitated with cx26 and cx30. Cx30 antibody recognises a protein of approximately 30 kDa in membrane preparations solubilised DM and immunoprecipiated with cx26 antibody as well as those precipitated with cx30 antibody. In preparations solubilised with SDS to dissociate connexons, cx30 antibodies recognise a protein only in the samples precipitated with cx30. **B:** Cx26 antibody labeling of Western blot of DM solubilised membrane proteins. The antibody recognises a protein of approximately 26 kDa in sample precipitated with cx30 as well as that precipitated with cx26.

DISCUSSION

Gap junction size and distribution

By using a combination of freeze fracture, confocal microscopy of connexin antibody-labeled tissues, and immunogold labeling for connexins in thin sections, we have analysed the sizes and distribution of gap junctions in sensory epithelia of the inner ear and in the lateral wall of the cochlea. Such a combined approach is required for an accurate assessment. Confocal microscopy of connexin-labeled tissue can provide information on the distribution of gap junctions, but freeze fracture provides a more accurate image of gap junction sizes. Many junctions are very small and may be below the level of resolution with confocal microscopy, and relatively close packing of small junction plaques can result in artefactual images on confocal microscopy suggesting that junctions are less numerous but much larger than they actually are. This is particularly apparent in examinations of Deiters cells, where freeze fracture and immunogold images show large numbers of closely arranged plaques, but confocal images often suggest a few large junctions surrounding the cell body. Likewise, among the basal cells of the stria vascularis, confocal imaging of immunolabeled tissue fails to resolve individually the numerous small junctions between basal cells and those between basal cells and intermediate cells.

The results show that gap junctions in the inner ear in all vertebrates are extremely numerous and often unusually large. In several cell types, gap junctions make up a significant proportion of the plasma membrane area, and, in the majority of the different tissues that make up the inner ear, all cells are extensively coupled to their neighbours. Potentially, large functional syncitia may extend throughout the entire cochlea or vestibular organs. The significant exception from gap junctional coupling is the sensory cells themselves. We could find no evidence of gap junction plaques on plasma membrane fracture faces of cells identified as hair cells by the characteristic complex network of tight junctional strands at their apical ends, the synaptic specialisations at the basal pole, or the presence of stereocilia in any of the species or sensory organs examined. Preliminary dye transfer studies of intact organs of Corti (D. Jagger and A. Forge, unpublished) have also shown that neither Lucifer yellow nor neurobiotin microinjected into supporting cells passes into hair cells, and photobleaching of calcein-AM-loaded explant cultures of chicken utricles and of basilar papillae have shown that the calcein-AM subsequently passes from the unbleached region into supporting cells in the bleached area but not into hair cells in that area (R. Nickel, D. Becker, and A. Forge, in preparation). These observations indicate that, at least in birds and mammals, hair cells are not functionally coupled to their neighbouring cells. The absence of gap junctional communication between hair cells and supporting cells presumably would allow each hair cell to function as an independent unit. However, others have reported from morphological studies the presence of gap junctions associated with hair cells in the auditory and vestibular organs of the alligator lizard (Nadol et al., 1976; Mulroy et al., 1993) and some species of fish (Hama, 1980). Determining whether this represents particular functional differences in these species from any of those studied here or is a consequence of misidentification will require studies of electrical or dye coupling of hair cells and supporting cells in these animals.

In addition, in the mammalian cochlea, the marginal cells of the stria vascularis do not form gap junctions either with their marginal cell neighbours or, in confirmation of results reported by Kikuchi et al. (1994), with the intermediate or basal cells with which marginal cells also make contact. Neither freeze fracture nor immunolabeling for connexins revealed gap junctions between the cell bodies of marginal cells or at sites of contact between marginal and intermediate cells. Furthermore, in thin sections for immunogold labeling in which preparation conditions had led to the separation of the tips of the basal projections of marginal cells from the basal cell, there was

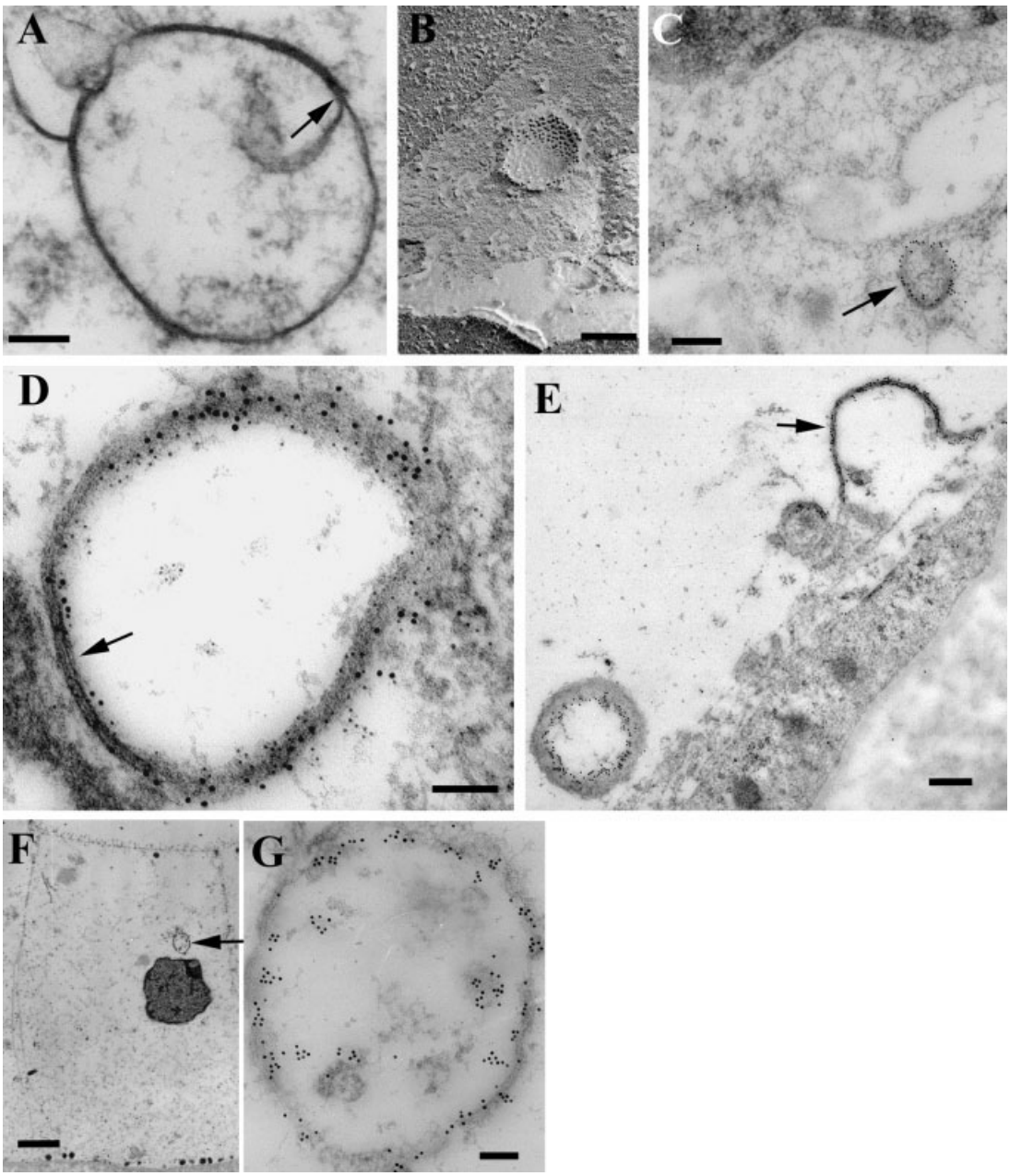

Fig. 12. Annular gap junctions. **A:** Double-membraned vesicle in inner sulcus cell of mouse with morphological features of a gap junction plaque in conventional thin section. The arrow indicates separation of the two membranes. **B:** Freeze fracture. Closely packed particles identical to those of a gap junction plaque on the membrane face of a vesicle inside a basal cell of the stria vascularis in gerbil. **C:** Membrane of vesicle (arrow) labeled for cx26 inside a fibrocyte of the spiral ligament in immunogold labeled thin section. **D:** Membrane-bound vesicle inside a Hensen cell doubly labeled for cx26 (5-nm gold particles) and cx30 (10-nm gold; polyclonal antibodies on opposite faces of section from mouse). The vesicle membrane is labeled in its entirety and evenly for both connexins. The arrow indicates where the vesicle membrane is cross-cut, revealing gap junction-like morphology and labeling for both connexins on both sides of the membrane profile. **E:** Membrane invagination (arrow) and closed, spherical vesicle close to the plasma membrane gold-labeled for connexins. **F:** Vesicle (arrowed) close to the nucleus in an inner sulcus cell. **G:** Vesicle with arrow in F at higher power, revealing labeling for connexin (cx26) all around the membrane but also labeling in material inside. Scale bars = 100 nm in A,B,D; 0.2 μmin C,E; 2 μm in F; 0.1 μm in G.

never any immunogold labeling on the tips of the marginal cell processes, and no plaques were seen on the membrane faces of these tips in freeze-fracture replicas. Thus, marginal cells, as with hair cells, appear to be functionally separated from each other and from their neighbouring cell types. The functional separation of marginal cells from either intermediate or basal cells may be crucial to the mechanisms by which EP is generated (Wangemann, 2002; discussed below). There may be other individual cell types that also are not coupled to their neigbours, and

neither gap junction plaques nor connexin labeling was detected in Reissner's membrane of the mammalian cochlea, but the majority of cell types in the inner ear do appear to be part of one or another coupled system.

Remarkably large gap junctions, often with over 100,000 channels and among the largest in the body, seem to be a feature of inner ear sensory epithelia in all vertebrates. In the supporting cells in all these tissues, there appears to be a common pattern of distribution of gap junctions. Numerous small plaques are present toward the lumenal side, but there are much larger plaques around the cell bodies. Although this pattern is particularly marked in some cells of the organ of Corti, most notably the inner pillar cells, the mammalian cochlea does not appear to be especially unusual in this respect vis á vis the vestibular sensory tissues or the sensory epithelia of other vertebrates, so it is not merely architectural constraints that impose a pattern of coupling and junction size on the organ of Corti. The presence of such a pattern of distribution and the extremely large size of the junctions between supporting cells in both the cochlear and the vestibular sensory epithelia of all vertebrates suggest that these features are in some way related to the particular functioning of these epithelia.

Differences in the size of junction plaques, i.e., in the number of channels, might be expected to correspond to differences in permeability, with perhaps increased coupling between cells when there are larger plaques. However, the relationship between channel number and permeability might not be so simple. There have been estimates that the permeability through one large gap junctional plaque may in fact be less than that with the same number of channels distributed among several smaller plaques, perhaps owing to interference between ions, for example, attempting to pass through a larger plaque (Hall and Gourdie, 1995). As yet there seems to be no direct evidence for this, but the supporting cells of the inner ear may be suited to assessment of this distinction. In very preliminary work, using fluorescence recovery after photobleaching to examine the passage of calcein-AM into bleached supporting cells from their unbleached neighbours in chick basilar papilla, transfer at the apical ends of the cells appears to be faster than that in the cell body region (R. Nickel and A. Forge, unpublished), but this awaits detailed confirmation. Nevertheless, it seems reasonable to suppose that there might be a functional correlate of the differential plaque size between the lumenal and the basal aspects of the supporting cell.

Additionally, if the size and number of plaques are a reflection of coupling efficiency between cells, then the difference in the size and number of basal cell–intermediate cell junctions in bats in comparison with the other mammalian species studied is of note. The cochleae in echo-locating bats, such as *Pteronotus parnellii*, are capable of unusually sharp frequency tuning within the ultrasonic frequency range, necessary for echo location, and show several morphological specialisations that are associated with this functional capacity (Vater and Kossl, 1996; Kossl and Vater, 1996). In the moustached bat, strial basal cells appear to have far more but smaller junctions than do those of the other mammals studied. Perhaps this contributes to the maintenance of frequency discrimination during echo detection by enhancing coupling efficiency between cells in the lateral wall. Certainly this suggests that gap junctional communication is tailored to the particular functional requirements of the tissues and emphasises the likely importance of gap junctions in the maintenance of auditory sensitivity.

Although there seem to be differences in the size of plaques down the depth of the supporting cells, in the vestibular sensory organs and the basilar papillae of lizards and birds, there is no obvious asymmetry in the distribution of gap junction plaques around supporting cells in the plane of the epithelium. Every supporting cell is coupled to all its neighbours potentially providing equal transfer in all directions. In the organ of Corti, there is, however, some asymmetry in the potential directions of coupling between supporting cells that reflects the architecture of the tissue. Cells in the inner sulcus and in those to the outside of the region of outer hair cells and Deiters cells appear to be coupled to all their neighbours in both radial and longitudinal directions. Deiters cells too are coupled to all their neighbours, providing potential communication pathways both radially and longitudinally, and there is no obvious difference in gap junction size or number around the Deiters cell body. In the pillar cell region, however, coupling would appear to be in the longitudinal direction along the organ of Corti in the cell body region through very large gap junction plaques but radial at the apical side between inner and outer pillar cells through much smaller plaques. There may also be radial coupling at the feet between outer and inner pillar cells; outer pillar cells are distinctly coupled radially to the innermost Deiters cell, and inner pillar cells are also coupled radially to the inner border cells. As suggested initially by Kikuchi et al. (1994), the radial coupling pathways could potentially provide a route for the recycling of K^+ ions away from the hair cells and out to the perilymph. However, longitudinal coupling pathways that would provide means to redistribute ions along the organ of Corti seem to be as extensive as those running radially.

Analysis of gap junction distribution in the lateral wall of the mammalian cochlea agrees with that previously reported (Kikuchi et al., 1995; Forge et al., 1999) and incorporated into models of how endocochlear potential is generated (Wangemann, 2002). Strial intermediate and basal cells, together with fibrocytes of the spiral ligament, form a coupled unit from which, as pointed out above, the strial marginal cells are excluded. This coupled unit is considered to be crucial to the generation of EP, providing a route of entry through the gap junctions for K^+ into the intermediate cells from perilymph that bypasses the extensive tight junctional sealing between basal cells (Forge, 1981, 1984), with EP generated across the plasma membrane of the intermediate cell (Wangemann, 2002). There is as yet no direct evidence that gap junctions function in this way in a K^+-recycling pathway, although during development the onset and rise of EP coincide with the formation and increase in size and number of gap junction plaques on the basal cell plasma membrane (Souter and Forge, 1998). However, it is also noteworthy that basal cells appear to be extensively coupled together not only in the direction to allow passage from ligament fibrocytes into the stria (radially) but also longitudinally along the cochlea. This, as with longitudinal coupling in the organ of Corti, raises the question of whether there is regulation of gap junction channels to modulate the communication pathways to suit particular physiological conditions.

Connexin expression in the mammalian inner ear

Analysis of which connexins are expressed in the inner ear and how they are distributed will aid in understanding cell coupling characteristics and regulation of intercellular communication. There is already evidence that several different connexins may be expressed in the inner ear; as pointed out in the introductory paragraphs, mutations in the genes for several different connexins have been reported to have adverse effects on auditory function. We sought to determine which connexins are expressed in the inner ear and how they are distributed. We tested for the presence in the mature inner ear of 12 of the 19 connexin isotypes that have been identified in the mouse genome. We have identified cx26, cx30, and cx43 and found evidence for cx31 and mRNA for cx50.

Cx32 was not identified in the mature inner ear. Neither the mRNA nor the protein was detected using Western blotting or immunohistochemstry with several different specific antibodies in conjunction with a variety of fixation protocols. We have also failed to detect cx32 in the developing inner ear (J. Edwards and A. Forge, unpublished). This suggests that the deafness associated with CMTX (Kousseff et al., 1982; Hamiel et al., 1993) is not due to defects at the auditory periphery. Mutations in cx32 that result in CMTX are thought to affect "reciprocal" gap junctions linking layers of the myelin sheaths in individual Schwann cells (Scherer et al., 1999) . There was no labeling for cx32 in the myelinated portions of the auditory nerve in the cochlea, nor have we been able to detect gap junction plaques in these regions of the cochlea by freeze fracture. Thus, the effects of cx32 mutations on hearing must occur somewhere farther up the auditory pathway.

Although mRNA for cx50 was detected, Western blotting provided only a faint band with an antibody that produced significant signal with lens tissue in which cx50 is highly expressed (White et al., 1992; Gong et al., 1997). Furthermore, immunohistochemical labeling failed to resolve specific cx50 immunoreactivity in the mature inner ear. We have obtained evidence for cx50 expression in localised regions of the inner ear during embryonic development in transgenic mice with targeted replacement of the cx50 gene with a lac-Z reporter (Gong et al., 1997), but expression is down-regulated before maturity (J. Edwards, N. Kumar, N.B. Gilula, and A. Forge, unpublished). The antibody used to label the mature tissue did provide some localised labeling in the immature cochlea and vestibular organs, suggesting that our failure to detect it in the mature cochlea is because cx50 is not expressed in the mature inner ear or, if it is, that it is not a major connexin component of inner ear tissues.

A previous study of cx31 (Xia et al., 2000) showed immunoreactivity in mouse inner ears in distinct regions of the lateral wall of the cochlea, among the type II fibrocytes of the mesenchymal tissue below the spiral prominence, but it was not detected in the fibrocytes below the stria vascularis, in the stria vascularis itself, or in the organ of Corti. However, in a transgenic mouse with targeted replacement of cx31 with Lac-Z reporter, no X-gal labeling was found in the cochlea either during embryonic development or in the mature tissues (Plum et al., 2001). No cx31 immunoreactivity was detected in the rat cochlea either (Lautermann et al., 1998). We found cx31 transcripts in cochlea but not vestibular tissue but found localisation of cx31 protein to be difficult. We used well-characterised cx31-specific antibodies obtained from Prof. K. Willecke (Butterweck et al., 1994) as well as a commercial antibody similar to that used by Xia et al. (2000). Weak positive immunoreactivity was obtained in the cochlea only in ethanol-fixed tissue in mice. A similar result was obtained with paraformaldehyde-fixed guinea pig tissue with an anti-human cx31 antibody obtained from Dr. D. Kelsell. Cx31 labeling was confined to only a subpopulation of fibrocytes. Because more intense labeling for cx31 was apparent in regions to the outside of the neonatal organ of Corti after maintenance of explants that included part of the lateral wall in organotypic culture, and examination of the cochleae of cx31 "knockout" mice, obtained from Prof K Willecke, revealed no labeling for cx31, we believe that our result probably represents a positive response to cx31 antibody in the mature cochlea. Thus, our results would support, at least partially, those of Xia et al. (2000), although further analysis of cx31 is perhaps warranted.

We found cx43 labeling in the mature cochlea to be confined to cells lining the otic capsule, in the marginal region of the spiral ligament and extending down into the lining of the scala tympani, with a crest of labeled cells protruding toward the basilar membrane. These cells would appear to correspond to the "tension" fibrocytes (Kuhn and Vater, 1997) that have been suggested to play a role in anchoring the spiral ligament and perhaps also exerting mechanical stress on the basilar membrane. However, unlike the case in previous reports (Lautermann et al., 1998; Liu et al., 2001), we did not detect cx43 in the organ of Corti nor in other regions of fibrocytes. In the vestibular system, cx43 immunoreactivity was present in a location equivalent to that in the cochlea, lining the walls of the vestibular canals, but punctate labeling for cx43 was also evident in the sensory epithelium of the vestibular organs. We do not know why our localisation of cx43 in the mature cochlea differs from that reported by others, although it is apparent that cx43 antibodies can be somewhat capricious. We used a variety of fixation protocols with several different antibodies, all of which provided positive labeling in some other tissue. None labeled in the mature organ of Corti, but labeling for cx43 was apparent quite widely in the developing cochlea, including the developing sensory region (J. Edwards and A. Forge, unpublished), but its expression was down-regulated with cochlear maturation. Our results therefore would suggest that cx43 is confined to a particular subset of cells in the mature cochlea and that the organ of Corti and vestibular sensory epithelia differ with respect to expression of cx43. It may be of note in this context that the initial report of deafness as a consequence of mutations in cx43 (Liu et al., 2001) has subsequently been attributed to erroneous identification of a pseudogene (Paznekas et al., 2003).

Cx26 and cx30, on the other hand, are both widely expressed in the inner ear. In the vestibular system, both connexins are present in the sensory epithelia and in the underlying connective tissue. In the cochlea, both connexins are present within the organ of Corti, in the fibrocytes of the spiral ligament beneath the stria vascularis, and in the basal cell layer of the stria itself. Not only do cx26 and cx30 appear to be present in the same tissues, the pattern of labeling suggests that they are colocalised. We have shown by Western blotting and by immunohistochemistry

of cell cultures expressing specific connexins that the antibodies to these two connexins do not cross-react and are isoform specific. Thus, the finding, from immunogold labeling with these characterised antibodies, that individual gap junction plaques throughout those areas where colocalisation is apparent are labeled for both connexins indicates that both connexins can be present in the same gap junction plaques. The labeling for each of the connexins was always even along the junction profiles on both sides of the junction. Such a pattern of labeling is consistent with individual connexons being heteromeric, containing both cx26 and cx30. Alternatively, there may be individual homotypic cx26 and cx30 connexons distributed through the plaques. However, we have recently found from in vitro experiments, expressing connexins in communication-deficient HeLa cells, that cx26 and cx30 can form heteromeric channels (Marziano et al., 2003). In addition, the present findings from coimmunoprecipiation experiments demonstrate that heteromeric cx26/cx30 connexons are present in the cochlea at least. We suggest, therefore, that such heteromeric channels are present in the organ of Corti and lateral wall tissues of the mammalian cochlea and in the sensory epithelia of the mammalian vestibular organs.

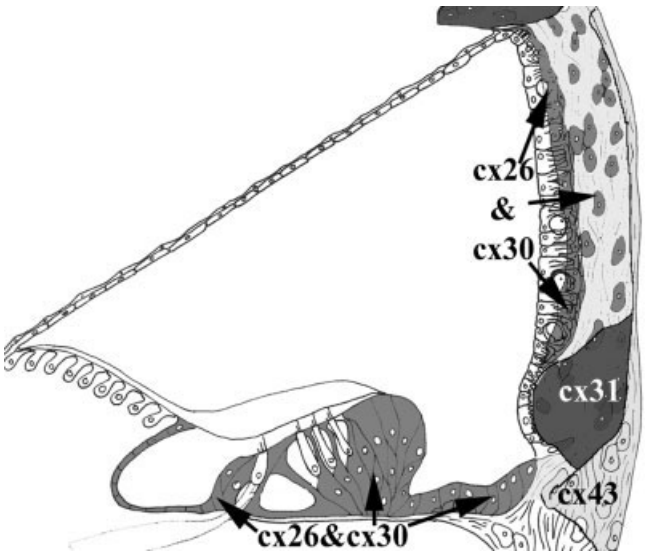

Fig. 13. Diagram of cross-section of cochlear duct indicating the localisation of the different connexins.

Annular gap junctions

Gap junctions are dynamic structures. There is evidence that connexins turn over rapidly, with half lives of 2–5 hours (Paulson et al., 2000; Evans and Martin, 2002). Recent imaging studies of cultured cells have also shown that newly produced connexons are constantly added at the edges of gap junction plaques, with preexisting ones in the centre removed to the cytoplasm (Falk, 2002; Gaietta et al., 2002; Lauf et al., 2002). In addition, it is thought that entire gap junction plaques can be internalised, creating "annular gap junctions," intracellular vesicular structures whose membranes contain connexons, which may then be degraded (Severs et al., 1989; Jordan et al., 2001). We found evidence for the presence of annular gap junctions in many cell types in the cochlea. They were particularly evident in immunogold-labeled thin sections where the labeling showed that the membranes of intracellular vesicles contained both of the connexin types identified in gap junction plaques, cx26 and cx30. It was also possible to identify an apparent progression in their formation from the labeling along the membranes. Segments of plasma membrane containing connexins were invaginated. Spherical vesicles with membranes labeled for connexins at a density exactly the same as that in gap junction plaques were present close to the plasma membrane. These were identified as intracellular vesicles rather than cross-sections of membrane invaginations from examination of several adjacent sections. Vesicles with connexin-labeled membranes were also present close to the nucleus. These vesicles were often less regular in outline than those closer to the plasma membrane, and the labeling was evident on amorphous material inside the vesicle as well as at the membrane, suggesting that degradation was occurring. The regularity with which annular gap junctions could be identified and the high number found in single thin sections indicate that their formation occurs extensively in the cochlea. This suggests a very rapid turnover of gap junctions.

The large size of many gap junction plaques indicates a considerable metabolic investment by supporting cells in maintaining their gap junctions. It also suggests that, insofar as entire gap junction plaques appear to be internalised, there maybe extensive dynamic remodelling of the intercellular communication pathways. However, it is of interest that, although annular gap junctions were frequently observed in many cell types, they were not obvious in others; in particular, they were not seen in inner pillar cells. This might indicate differences in the mode or rate of turnover between cell types.

CONCLUSIONS

Taken together, our results lead to a number of suggestions. 1) Different connexin isotypes are present in separate subregions of the cochlea (Fig. 13): cx43 in the marginal regions of the ligament, where there is no cx26 or cx30; cx31 in a fibrocyte subpopulation, where there is little expression of cx30 or cx26; cx26 and cx30 are colocalised elsewhere. 2) Cx26 and cx30 are the only connexins expressed in the organ of Corti, in the basal cells of the stria vascularis and perhaps also in the fibrocytes beneath the stria vascularis. There are, of course, seven connexins in the mouse genome (one of which has no apparent human orthologue) and eight in that of humans (two of which have no mouse orthologues; Willecke et al., 2002) for which we have not screened. Analysis of these is necessary to confirm this conclusion. 3) The supporting cells of the vestibular sensory epithelia may contain cx43 in addition to cx26 and cx30, which those of the organ of Corti do not. 4) Cx26 and cx30 form heteromeric connexons. Such channels are likely to have unique properties different from those of cx26 alone or cx30 alone.

We have found, in the inner ear of chickens, positive immunoreactivity for cx26, cx30, and cx43 in both the utricular maculae and the basilar papilla (R. Nickel, D. Becker, and A. Forge, unpublished). From in vitro expression studies (R. Nickel and A. Forge, unpublished), the cx26/cx30 immunoreactivity appears to result from the presence of a particular chicken connexin, c-cx31 (different from mammalian cx31)

that is uniquely expressed in the inner ear of the chicken (Heller et al., 1998). C-cx31 has significant sequence similarity to cx26 throughout its length but with a c-terminal tail with sequence similarity to cx30, thus appearing to be almost a chimera of cx26 and cx30. Therefore, connexons composed of c-cx31 may have properties similar to those of heteromeric 26/cx30 connexons. This suggests that there maybe similarities in the connexins expressed in inner ear sensory epithelia across vertebrate classes but that the organ of Corti specialisation is associated with loss of cx43 expression. It may also suggest that the physiological properties of heteromeric channels containing cx30 and cx26, or the avian equivalent, are uniquely suited to the physiological demands of vertebrate mechanosensitive epithelia. Determining the properties of those channels is an area for future work.

If our interpretations are correct, then they could account for some of the clinical manifestations of cx26 mutations. It maybe that heteromeric cx26/cx30 channels are present only in inner ear tissues; that mutations in cx26 affect the functionality of such heteromeric channels; and that, in the absence of any other connexin, there is no possibility for compensation of defective connexins by others. If this were so, it could account for the nonsyndromic character of the deafness that results from many cx26 mutations. We have found in in vitro studies using a HeLa cell connexin-expression system that mutant proteins associated with dominant nonsyndromic deafness do indeed affect intercellular communication in cells coexpressing wild-type cx30 and mutant cx26 (Marziano et al., 2003). In addition, if the vestibular sensory epithelia express cx43 as well as cx26 and cx30 it may be that channels containing cx43 can compensate for functional deficiencies caused in those containing cx26. This could account for the apparent lack of vestibular dysfunction in patients who are deaf because of cx26 mutations. However, other explanations for the lack of a vestibular phenotype are possible. The disruption of intercellular communication may impair K^+ recycling and the ability to generate or maintain EP (Teubner et al., 2003). EP is essential for auditory function in mammals, but there is no equivalent in the vestibular system. Therefore, the vestibular organs may be less dependent on efficient cell–cell coupling. Impairment of intercellular communication may also have a more generalised detrimental effects on cochlear homeostasis, to which the organ of Corti is particularly sensitive. Mutations in several different genes whose products appear to be involved in maintenance of cochlear homeostasis cause nonsyndromic deafness and death of outer hair cells (Steel and Kros, 2001), suggesting that the organ of Corti may be particularly sensitive to its ionic environment, and targeted deletion of the cx26 gene from organ of Corti and vestibular supporting cells or expression of a dominant negative cx26 mutation (Kudo et al., 2003) also leads to death of outer hair cells (Cohen-Salmon et al., 2002), with no obvious effects in vestibular organs.

ACKNOWLEDGEMENTS

We are grateful to all those colleagues who supplied antibodies, especially to the late Prof. Bernie Gilula and his laboratory members at the Scripps Research Institute, who also assisted with Western blotting, and to those who provided inner ears from the various species.

LITERATURE CITED

Bitner-Glindzicz M. 2002. Hereditary deafness and phenotyping in humans. Br Med Bull 63:73–94.

Boettger T, Hubner CA, Maier H, Rust MB, Beck FX, Jentsch TJ. 2002. Deafness and renal tubular acidosis in mice lacking the K-Cl cotransporter Kcc4. Nature 416:874–878.

Bruzzone R, White TW, Paul DL. 1996. Connections with connexins: the molecular basis of direct intercellular signaling. Eur J Biochem 238:1–27.

Butterweck A, Elfgang C, Willecke K, Traub O. 1994. Differential expression of the gap junction proteins connexin45, -43, -40, -31, and -26 in mouse skin. Eur J Cell Biol 65:152–163.

Carlisle L, Steel K, Forge A. 1990. Endocochlear potential generation is associated with intercellular communication in the stria vascularis: structural analysis in the viable dominant spotting mouse mutant. Cell Tissue Res 262:329–337.

Carrasquillo MM, Zlotogora J, Barges S, Chakravarti A. 1997. Two different connexin 26 mutations in an inbred kindred segregating nonsyndromic recessive deafness: implications for genetic studies in isolated populations. Hum Mol Genet 6:2163–2172.

Cohen-Salmon M, Ott T, Michel V, Hardelin JP, Perfettini I, Eybalin M, Wu T, Marcus DC, Wangemann P, Willecke K, Petit C. 2002. Targeted ablation of connexin26 in the inner ear epithelial gap junction network causes hearing impairment and cell death. Curr Biol 12:1106–1111.

Davies TC, Barr KJ, Jones DH, Zhu D, Kidder GM. 1996. Multiple members of the connexin gene family participate in preimplantation development of the mouse. Dev Genet 18:234–243.

Denoyelle F, Weil D, Maw MA, Wilcox SA, Lench NJ, Allen-Powell DR, Osborn AH, Dahl HH, Middleton A, Houseman MJ, Dode C, Marlin S, Boulila-ElGaied A, Grati M, Ayadi H, BenArab S, Bitoun P, Lina-Granade G, Godet J, Mustapha M, Loiselet J, El-Zir E, Aubois A, Joannard A, Petit C, et al. 1997. Prelingual deafness: high prevalence of a 30delG mutation in the connexin 26 gene. Hum Mol Genet 6:2173–2177.

Elfgang C, Eckert R, Lichtenberg-Frate H, Butterweck A, Traub O, Klein RA, Hulser DF, Willecke K. 1995. Specific permeability and selective formation of gap junction channels in connexin-transfected HeLa cells. J Cell Biol 129:805–817.

Evans WH, Martin PE. 2002. Gap junctions: structure and function [review]. Mol Membr Biol 19:121–136.

Falk MM. 2000. Connexin-specific distribution within gap junctions revealed in living cells. J Cell Sci 113:4109–4120.

Falk MM. 2002. Genetic tags for labeling live cells: gap junctions and beyond. Trends Cell Biol 12:399–404.

Forge A. 1981. Electron microscopy of the stria vascularis and its response to etacrynic acid. A study using electron-dense tracers and extracellular surface markers. Audiology 20:273–289.

Forge A. 1984. Gap junctions in the stria vascularis and effects of ethacrynic acid. Hear Res 13:189–200.

Forge A. 1986. The morphology of the normal and pathological cell membrane and junctional complexes of the cochlea. New York: Plenum Publishing Corp.

Forge A, Becker D, Casalotti S, Edwards J, Evans WH, Lench N, Souter M. 1999. Gap junctions and connexin expression in the inner ear. Novartis Found Symp 219:134–150, discussion 151–136.

Forge A, Becker D, Casalotti S, Edwards J, Marziano N, Nickel R. 2002. Connexins and gap junctions in the inner ear. Audiol Neurootol 7:141–145.

Gaietta G, Deerinck TJ, Adams SR, Bouwer J, Tour O, Laird DW, Sosinsky GE, Tsien RY, Ellisman MH. 2002. Multicolor and electron microscopic imaging of connexin trafficking. Science 296:503–507.

Gilula NB, Reeves OR, Steinbach A. 1972. Metabolic coupling, ionic coupling and cell contacts. Nature 235:262–265.

Ginzberg RD, Gilula NB. 1979. Modulation of cell junctions during differentiation of the chicken otocyst sensory epithelium. Dev Biol 68:110–129.

Gong X, Li E, Klier G, Huang Q, Wu Y, Lei H, Kumar NM, Horwitz J, Gilula NB. 1997. Disruption of alpha3 connexin gene leads to proteolysis and cataractogenesis in mice. Cell 91:833–843.

Grifa A, Wagner CA, D'Ambrosio L, Melchionda S, Bernardi F, Lopez-Bigas N, Rabionet R, Arbones M, Monica MD, Estivill X, Zelante L, Lang F, Gasparini P. 1999. Mutations in GJB6 cause nonsyndromic autosomal dominant deafness at DFNA3 locus. Nat Genet 23:16–18.

Gulley RL, Reese TS. 1976. Intercellular junctions in the reticular lamina of the organ of Corti. J Neurocytol 5:479–507.

Hall JE, Gourdie RG. 1995. Spatial organization of cardiac gap junctions can affect access resistance. Microsc Res Techniq 31:446–451.

Hama K. 1980. Fine structure of the afferent synapse and gap junctions on the sensory hair cell in the saccular macula of goldfish: a freeze-fracture study. J Neurocytol 9:845–860.

Hamiel OP, Raas-Rothschild A, Upadhyaya M, Frydman M, Sarova-Pinhas I, Brand N, Passwell JH. 1993. Hereditary motor-sensory neuropathy (Charcot-Marie-Tooth disease) with nerve deafness: a new variant. J Pediatr 123:431–434.

Heller S, Sheane CA, Javed Z, Hudspeth AJ. 1998. Molecular markers for cell types of the inner ear and candidate genes for hearing disorders. Proc Natl Acad Sci U S A 95:11400–11405.

Hirokawa N. 1980. A freeze-fracture study of intercellular junctions between various kinds of epithelial cells surrounding common endolymphatic space in the hearing organ of the chick. Anat Rec 196:129–143.

Iurato S, Franke K, Luciano L, Wermbter G, Pannese E, Reale E. 1976. Intercellular junctions in the organ of Corti as revealed by freeze fracturing. Acta Otolaryngol 82:57–69.

Iurato S, Franke KD, Luciano L, Wermbter G, Pannese F, Reale E. 1977. The junctional complexes among the cells of the organ of Corti as revealed by freeze-fracturing. Adv Otorhinolaryngol 22:76–80.

Jahnke K. 1975. The fine structure of freeze-fractured intercellular junctions in the guinea pig inner ear. Acta Otolaryngol Suppl 336:1–40.

Jordan K, Chodock R, Hand AR, Laird DW. 2001. The origin of annular junctions: a mechanism of gap junction internalization. J Cell Sci 114:763–773.

Kelley PM, Cohn E, Kimberling WJ. 2000. Connexin 26: required for normal auditory function. Brain Res Brain Res Rev 32:184–188.

Kelsell DP, Dunlop J, Stevens HP, Lench NJ, Liang JN, Parry G, Mueller RF, Leigh IM. 1997. Connexin 26 mutations in hereditary non-syndromic sensorineural deafness. Nature 387:80–83.

Kikuchi T, Adams JC, Paul DL, Kimura RS. 1994. Gap junction systems in the rat vestibular labyrinth: immunohistochemical and ultrastructural analysis. Acta Otolaryngol 114:520–528.

Kikuchi T, Kimura RS, Paul DL, Adams JC. 1995. Gap junctions in the rat cochlea: immunohistochemical and ultrastructural analysis. Anat Embryol 191:101–118.

Kikuchi T, Kimura RS, Paul DL, Takasaka T, Adams JC. 2000. Gap junction systems in the mammalian cochlea. Brain Res Brain Res Rev 32:163–166.

Kossl M, Vater M. 1996. Further studies on the mechanics of the cochlear partition in the mustached bat. II. A second cochlear frequency map derived from acoustic distortion products. Hear Res 94:78–86.

Kousseff BG, Hadro TA, Treiber DL, Wollner T, Morris C. 1982. Charcot-Marie-Tooth disease with sensorineural hearing loss—an autosomal dominant trait. BDOAS 18:223–228.

Kudo T, Kure S, Ikeda K, Xia AP, Katori Y, Suzuki M, Kojima K, Ichinohe A, Suzuki Y, Aoki Y, Kobayashi T, Matsubara Y. 2003. Transgenic expression of a dominant-negative connexin26 causes degeneration of the organ of Corti and non-syndromic deafness. Hum Mol Genet 12: 995–1004.

Kuhn B, Vater M. 1997. The postnatal development of F-actin in tension fibroblasts of the spiral ligament of the gerbil cochlea. Hear Res 108: 180–190.

Kumar NM, Gilula NB. 1996. The gap junction communication channel. Cell 84:381–388.

Lauf U, Giepmans BN, Lopez P, Braconnot S, Chen SC, Falk MM. 2002. Dynamic trafficking and delivery of connexons to the plasma membrane and accretion to gap junctions in living cells. Proc Natl Acad Sci U S A 99:10446–10451.

Lautermann J, ten Cate WJ, Altenhoff P, Grummer R, Traub O, Frank H, Jahnke K, Winterhager E. 1998. Expression of the gap-junction connexins 26 and 30 in the rat cochlea. Cell Tissue Res 294:415–420.

Lautermann J, Frank HG, Jahnke K, Traub O, Winterhager E. 1999. Developmental expression patterns of connexin26 and -30 in the rat cochlea. Dev Genet 25:306–311.

Liu XZ, Xia XJ, Adams J, Chen ZY, Welch KO, Tekin M, Ouyang XM, Kristiansen A, Pandya A, Balkany T, Arnos KS, Nance WE. 2001. Mutations in GJA1 (connexin 43) are associated with non-syndromic autosomal recessive deafness. Hum Mol Genet 10:2945–2951.

Marziano NK, Casalotti SO, Portelli AE, Becker DL, Forge A. 2003. Mutations in the gene for connexin 26 (GJB2) that cause hearing loss have a dominant negative effect on connexin 30. Hum Mol Genet 12:805–812.

McGuirt JP, Schulte BA. 1994. Distribution of immunoreactive alpha- and beta-subunit isoforms of Na,K-ATPase in the gerbil inner ear. J Histochem Cytochem 42:843–853.

McNutt NS, Weinstein RS. 1970. The ultrastructure of the nexus. A correlated thin-section and freeze-cleave study. J Cell Biol 47:666–688.

Merchan-Perez A, Gil-Loyzaga P, Bartolome MV, Remezal M, Fernandez P, Rodriguez T. 1999. Decalcification by ascorbic acid for immuno- and affinohistochemical techniques on the inner ear. Histochem Cell Biol 112:125–130.

Mulroy MJ, Dempewolf SA, Curtis S, Iida HC. 1993. Gap junctional connections between hair cells, supporting cells and nerves in a vestibular organ. Hear Res 71:98–105.

Nadol JB Jr, Mulroy MJ, Goodenough DA, Weiss TF. 1976. Tight and gap junctions in a vertebrate inner ear. Am J Anat 147:281–301.

Paulson AF, Lampe PD, Meyer RA, TenBroek E, Atkinson MM, Walseth TF, Johnson RG. 2000. Cyclic AMP and LDL trigger a rapid enhancement in gap junction assembly through a stimulation of connexin trafficking. J Cell Sci 113:3037–3049.

Paznekas WA, Boyadjiev SA, Shapiro RE, Daniels O, Wollnik B, Keegan CE, Innis JW, Dinulos MB, Christian C, Hannibal MC, Jabs EW. 2003. Connexin 43 (GJA1) mutations cause the pleiotropic phenotype of oculodentodigital dysplasia. Am J Hum Genet 72:408–418.

Plum A, Winterhager E, Pesch J, Lautermann J, Hallas G, Rosentreter B, Traub O, Herberhold C, Willecke K. 2001. Connexin31-deficiency in mice causes transient placental dysmorphogenesis but does not impair hearing and skin differentiation. Dev Biol 231:334–347.

Schagger H, von Jagow G. 1987. Tricine-sodium dodecyl sulfate-polyacrylamide gel electrophoresis for the separation of proteins in the range from 1 to 100 kDa. Anal Biochem 166:368–379.

Scherer SS, Bone LJ, Deschenes SM, Abel A, Balice-Gordon RJ, Fischbeck KH. 1999. The role of the gap junction protein connexin32 in the pathogenesis of X-linked Charcot-Marie-Tooth disease. Novartis Found Symp 219:175–185, discussion 185–177.

Schulte BA, Steel KP. 1994. Expression of alpha and beta subunit isoforms of Na,K-ATPase in the mouse inner ear and changes with mutations at the Wv or Sld loci. Hear Res 78:65–76.

Severs NJ. 1990. The cardiac gap junction and intercalated disc. Int J Cardiol 26:137–173.

Severs NJ, Shovel KS, Slade AM, Powell T, Twist VW, Green CR. 1989. Fate of gap junctions in isolated adult mammalian cardiomyocytes. Circ Res 65:22–42.

Souter M, Forge A. 1998. Intercellular junctional maturation in the stria vascularis: possible association with onset and rise of endocochlear potential. Hear Res 119:81–95.

Stauffer KA, Kumar NM, Gilula NB, Unwin N. 1991. Isolation and purification of gap junction channels. J Cell Biol 115:141–150.

Steel KP, Kros CJ. 2001. A genetic approach to understanding auditory function. Nat Genet 27:143–149.

Teubner B, Michel V, Pesch J, Lautermann J, Cohen-Salmon M, Sohl G, Jahnke K, Winterhager E, Herberhold C, Hardelin JP, Petit C, Willecke K. 2003. Connexin30 (Gjb6)-deficiency causes severe hearing impairment and lack of endocochlear potential. Hum Mol Genet 12:13–21.

Vater M, Kossl M. 1996. Further studies on the mechanics of the cochlear partition in the mustached bat. I. Ultrastructural observations on the tectorial membrane and its attachments. Hear Res 94:63–77.

Veenstra RD. 1996. Size and selectivity of gap junction channels formed from different connexins. J Bioenerg Biomembr 28:327–337.

Wangemann P. 2002. K^+ cycling and the endocochlear potential. Hear Res 165:1–9.

White TW, Bruzzone R, Goodenough DA, Paul DL. 1992. Mouse Cx50, a functional member of the connexin family of gap junction proteins, is the lens fiber protein MP70. Mol Biol Cell 3:711–720.

Willecke K, Eiberger J, Degen J, Eckardt D, Romualdi A, Guldenagel M, Deutsch U, Sohl G. 2002. Structural and functional diversity of connexin genes in the mouse and human genome. Biol Chem 383:725–737.

Xia AP, Ikeda K, Katori Y, Oshima T, Kikuchi T, Takasaka T. 2000. Expression of connexin 31 in the developing mouse cochlea. Neuroreport 11:2449–2453.

Xia A, Katori Y, Oshima T, Watanabe K, Kikuchi T, Ikeda K. 2001. Expression of connexin 30 in the developing mouse cochlea. Brain Res 898:364–367.

Xia JH, Liu CY, Tang BS, Pan Q, Huang L, Dai HP, Zhang BR, Xie W, Hu DX, Zheng D, Shi XL, Wang DA, Xia K, Yu KP, Liao XD, Feng Y, Yang YF, Xiao JY, Xie DH, Huang JZ. 1998. Mutations in the gene encoding gap junction protein beta-3 associated with autosomal dominant hearing impairment. Nat Genet 20:370–373.